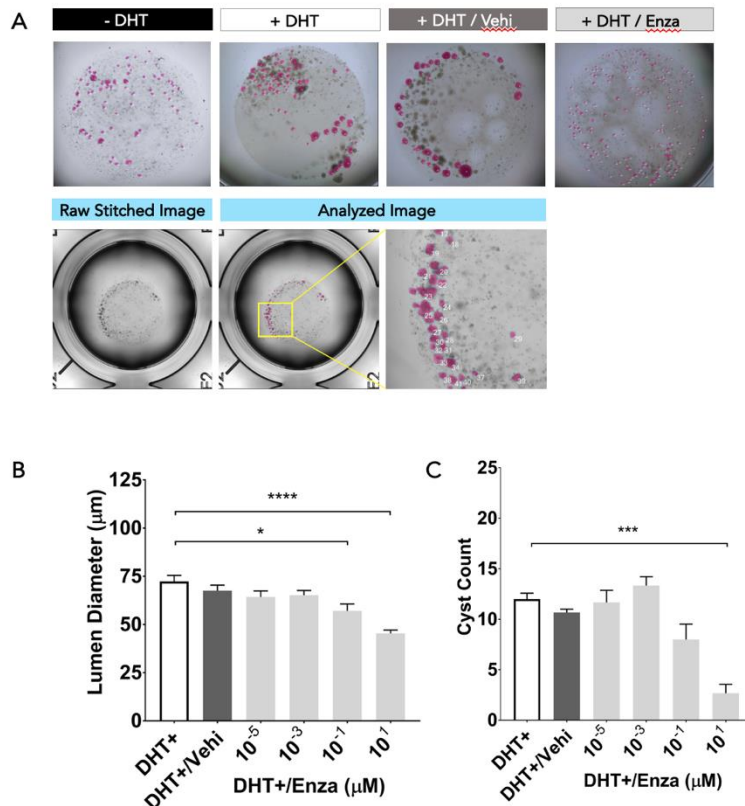
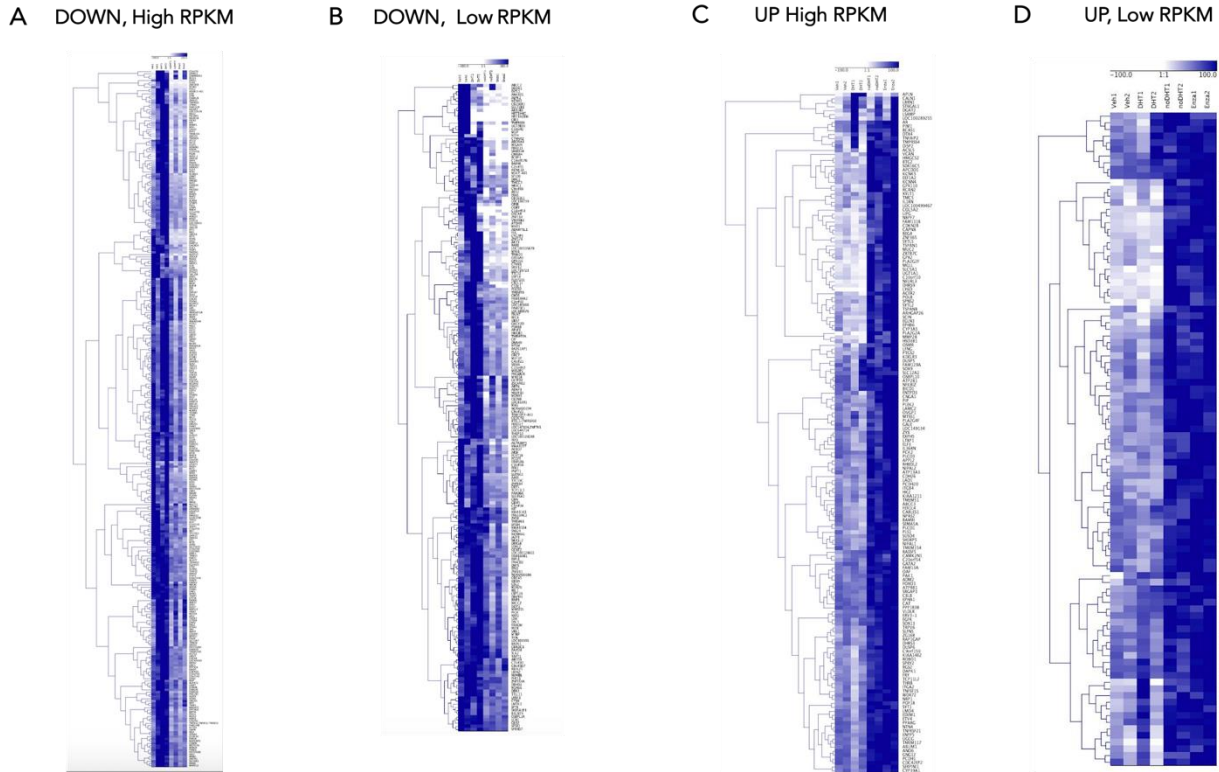


## Supplementary Materials



**Figure S1.** Digital microscope image of whole matrigel dome with spheroids outlined for area analysis. (A) Representative images of whole Matrigel domes of 3D organoid cultures with spheroids outlined in pink from the four treatment groups: -DHT, +DHT, +DHT/Vehicle, +DHT/Enzalutamide. Spheroid area was measured using the Keyence Hybrid Cell Counter at 4X magnification by outlining spheroid clusters (pink line) that were at least 50  $\mu\text{m}$  in size with the Free Draw Tool. PCSD1 Organoid cultures were treated with increasing concentrations of enzalutamide to determine the effect on (B) lumen diameter (in  $\mu\text{m}$ ) and (C) cyst count. Enzalutamide at 10  $\mu\text{M}$  showed significant reduction of cyst size and number and was used in subsequent experiments. Data represent the mean from two ( $n=2$ ) experiments  $\pm$  SEM. A student's t-test was used to determine statistical significance (\*\* indicates  $P < 0.01$ ). GFP fluorescence was measured using the Keyence BZX 710 microscope (Keyence Corporation) on a weekly basis.



**Figure S2.** Hierarchical Clustering Analysis of Gene Expression Profiles from PDX Organoids under APDT. Heatmaps organized by hierarchical clustering analysis for differentially expressed genes in PCSD1 organoids under two androgen treatment conditions (1) Veh (+DHT/Vehicle – 1 nM/0.1% DMSO), (2) DHT (+DHT – 1 nM) and PCSD1 organoids under two androgen deprivation treatment conditions: (3) noDHT (-DHT) and (4) Enza (+DHT/Enzalutamide – 1 nM/1uM). Genes presented in four groups: (A) down-regulated under APDT, high normalized read counts (RPKM), (B) down-regulated under APDT, low RPKM, (C) up-regulated under APDT, high RPKM, and (D) up-regulated under APDT, low RPKM. To identify genes responsive to androgen deprivation, a series of queries were applied to the read count tables. First, queries identified genes with expression change in the same direction in both experiments 1 and 2 under Enzalutamide treatment (Enza) compared to vehicle treatment (+DHT/Veh). To focus on highly responsive genes, a minimal threshold change of  $\text{abs}(\log_2(\text{Enza}/\text{Veh})) > 0.75$  was required for a gene change to be considered "UP"- or "DOWN"-regulated by androgen deprivation or anti-androgen. Genes with changes below this threshold were set aside. Next, genes were ranked according to change between treatment with Enzalutamide versus noDHT, with lower values for  $\text{abs}(\log_2(\text{Enza}/\text{noDHT}))$  ratios ranked higher. Filtered genes were then split into two groups for further evaluation and ranking: genes with all RPKM read counts below 10 were considered as low expression genes (Low), and the rest as higher expression genes (High), resulting in four groups of genes for pathway analysis: UP, Low RPKM (98 genes); DOWN, Low RPKM (206 genes); UP, High RPKM (171 genes); DOWN, High RPKM (312 genes).

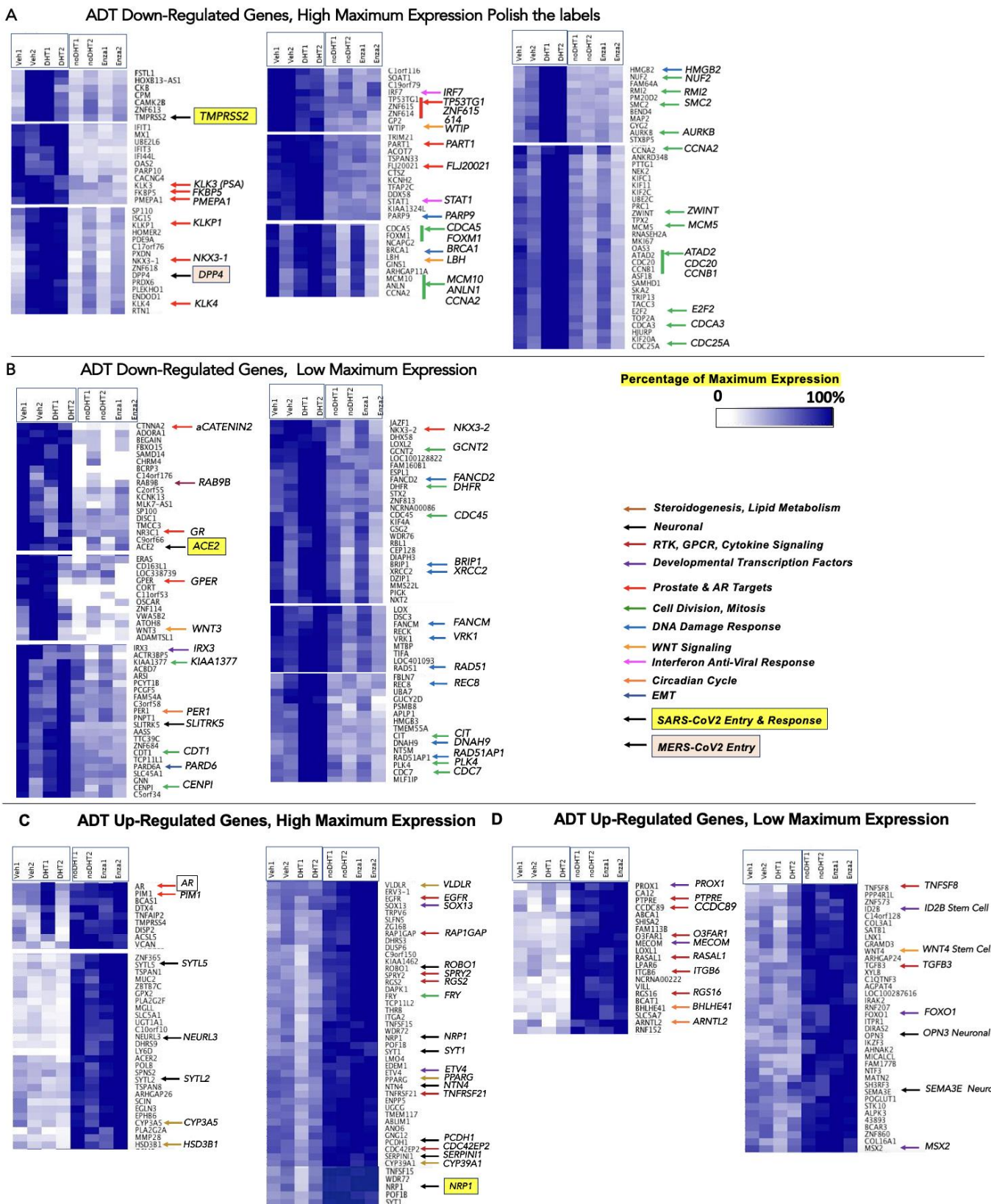


**Figure S3.** Comparative Gene Expression Profiling of APDT Treatment in PDOs. Hierarchical clusters were selected which show consistent gene expression changes between different androgen signaling conditions from whole genome bulk RNASeq analysis. Gene expression is displayed as percentage of maximum normalized reads per kilobase of transcript per million mapped reads (RPKM). Increase intensity of blue indicates increasing mRNA expression level while increasing white represents decreasing mRNA expression. (A) Significantly down-regulated genes with high normalized read counts (RPKM). Genes from functional categories enriched in the differential genes marked with arrows: prostate & AR targets (red); cell division, mitosis (green); DNA damage response (blue); WNT signaling (orange); interferon anti-viral response (pink); SARS-CoV-2 entry & response (black arrow with yellow box) and MERS-CoV entry (black arrow with beige box). (B) Significantly down-regulated genes with low overall RPKM. Genes from

functional categories enriched in the differential genes marked with arrows: steroidogenesis, lipid metabolism (brick red); neuronal (black); RTK, GPCR, cytokine signaling (red); developmental transcription factors (purple); prostate & AR targets (bright red); cell division, mitosis (green); DNA damage response (blue); WNT signaling (light orange); interferon anti-viral response (pink); circadian cycle (orange); EMT (dark blue) and SARS-CoV-2 entry & response (black arrow with yellow box). Data represent the mean from four independent (n=4) experiments performed in triplicate ± SEM. (C) Significantly up-regulated genes with high normalized read counts (RPKM). Genes from functional categories enriched in the differential genes marked with arrows: steroidogenesis, lipid metabolism (brick red); neuronal (black); RTK, GPCR, cytokine signaling (brown); developmental transcription factors (purple); prostate & AR targets (red); cell division, mitosis (green); DNA damage response (blue); WNT signaling (orange); interferon anti-viral response (pink); circadian circle (dark orange) and SARS-CoV-2 entry & response & pain (black arrow with yellow box). (D) Significantly up-regulated genes with low overall RPKM. Genes from functional categories enriched in the differential genes marked with arrows: steroidogenesis, lipid metabolism (brick red); neuronal (black); RTK, GPCR, cytokine signaling (dark brown); developmental transcription factors (purple); prostate & AR targets (bright red); cell division, mitosis (green); DNA damage response (blue); WNT signaling (light orange); interferon anti-viral response (pink) and circadian cycle (orange). Data represent the mean from four independent (n=4) experiments performed in triplicate ± SEM.

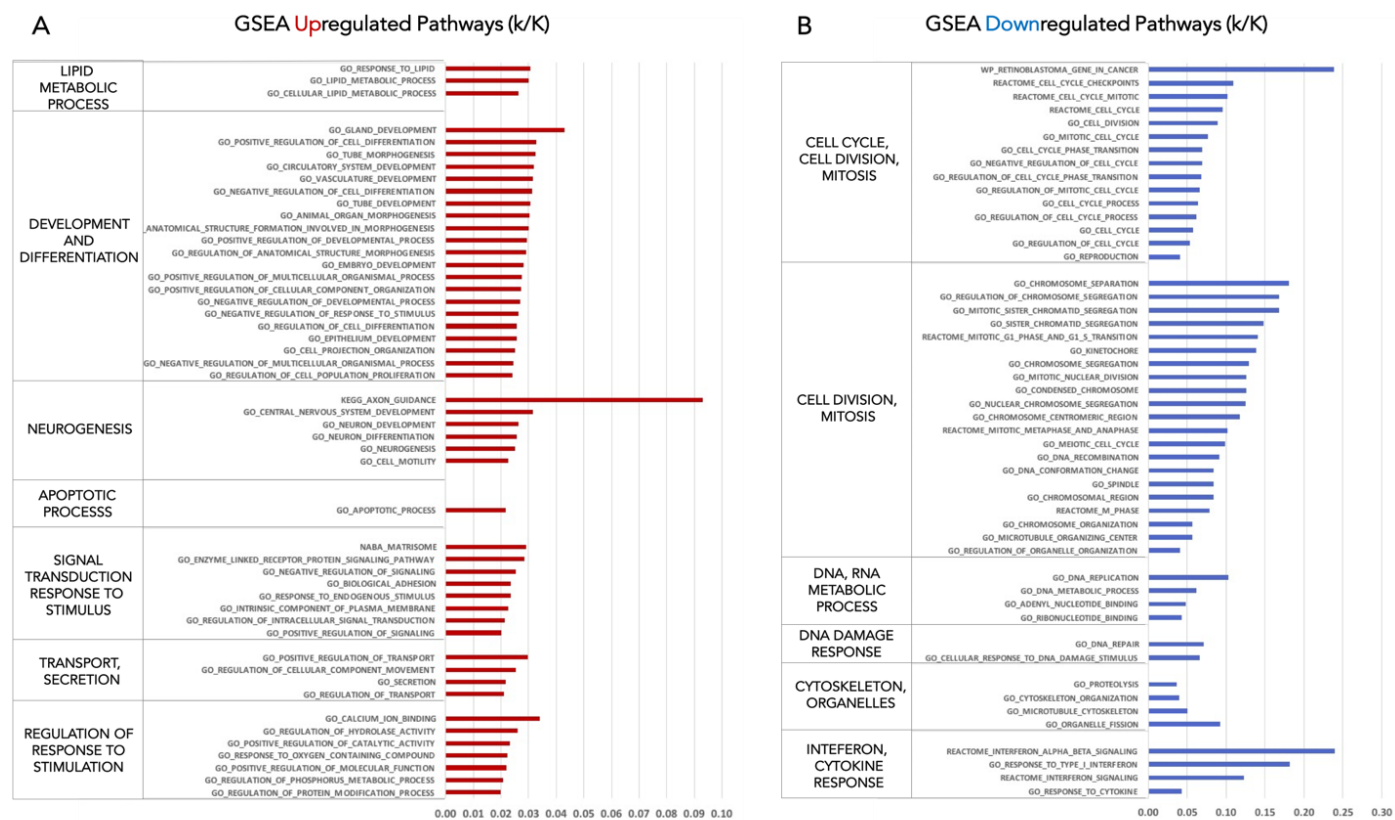


**Figure S4.** Gene Sets Revealed as Enriched in Differentially Expressed Genes Using Gene Set Enrichment Analysis (GSEA). (A) Enriched GSEA gene sets for genes up-regulated under APDT (red). (B) Enriched GSEA gene sets for genes down-regulated under APDT (blue). GSEA evaluates enrichment for sets of genes (gene sets) derived from multiple databases and from many experiments with data deposited in public, curated repositories and reported in the literature. Since many gene sets overlap and share a functional category theme, overlapping gene sets were downloaded from GSEA and merged to create curated sets of genes for functional categories with highly differential key regulatory genes: Interferon Signaling (102 genes), Cell Cycle (2038 genes), Circadian Clock (240 genes), Neurogenesis (1701 genes), Axon Guidance (129 genes; evaluated as a subset of Neurogenesis), Hormone Response (529 genes; including glucocorticoid response), and Steroid Receptor Signaling (385 genes). Two additional lists of genes were derived through literature review: Prostate Stem/Progenitor (96 genes) and Neuro-Endocrine Prostate Cancer (NEPC)/Neurogenic (269 genes). Gene lists for NEPC/neurogenic and prostate stem/progenitor categories were generated from the literature[73-90]. Figure S5 provides lists of GSEA pathways enriched in significantly up-regulated genes and significantly down-regulated genes. Enriched pathways for up-regulated genes include lipid metabolic process, development, differentiation, neurogenesis, apoptotic process, signal transduction response to stimulus, transcription, secretion and regulation of response to stimulation. Enriched pathways for down-regulated genes include cell cycle, cell division, mitosis, DNA/RNA metabolic process, DNA damage response, cytoskeleton, organelles, interferon and cytokine response.

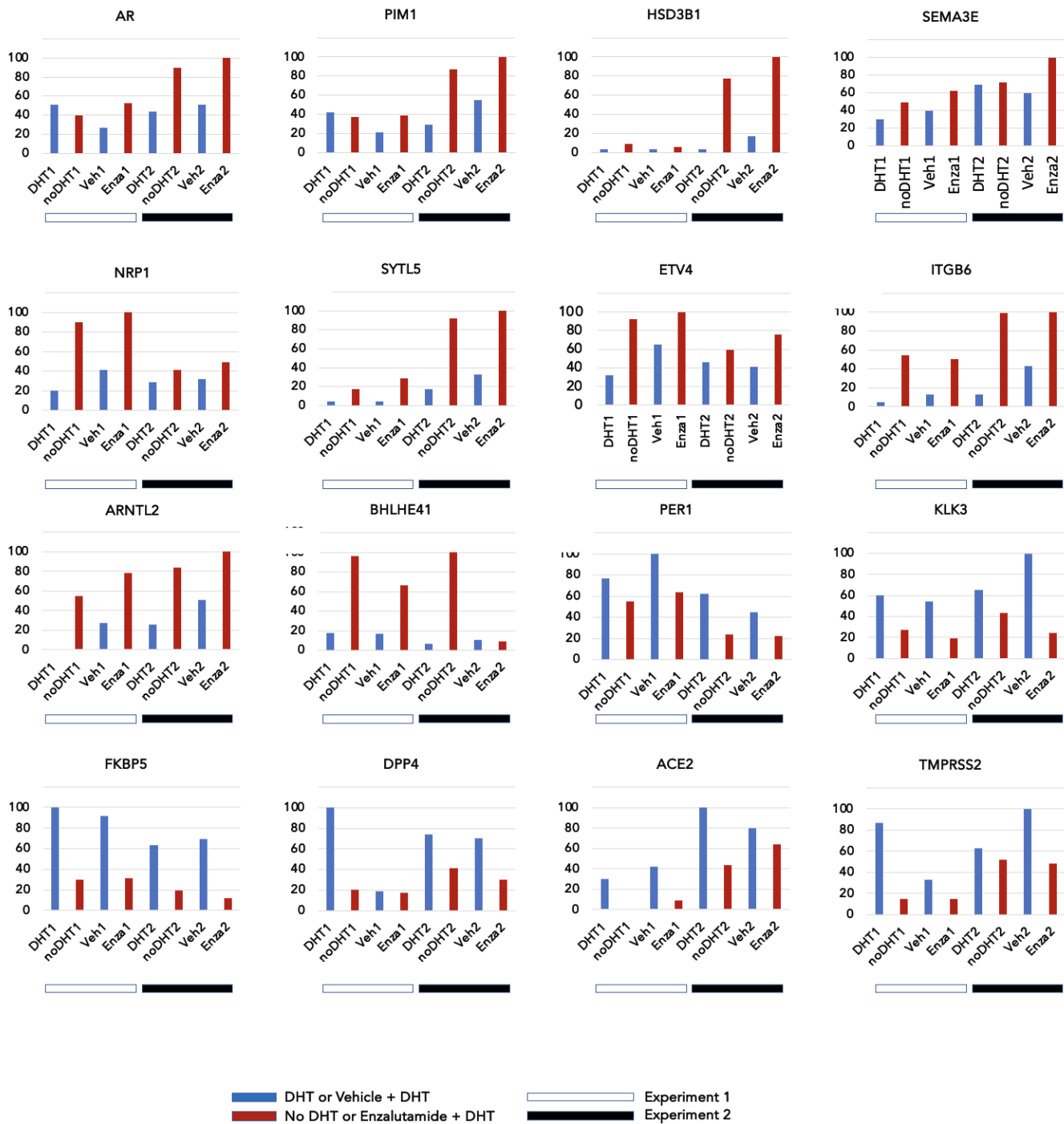


**Figure S5.** Comparison of Expression Levels of Individual Genes of Interest in ADT-treated PDOs. Comparisons of gene expression for selected genes of interest under different androgen signaling conditions are shown as bar graphs of percentage of maximum RPKM observed for each gene. Blue bars are PCSD1 organoid samples treated with 1nM DHT or Vehicle (0.1%DMSO) + 1nM DHT. Red bars are PCSD1 organoid samples treated with No DHT or 10 $\circ$ M Enzalutamide + 1nM DHT. Samples from Experiment 1 are shown on the left with white horizontal bar along X-axis and samples from Experiment 2 are shown on the right with black horizontal bar along X-axis.

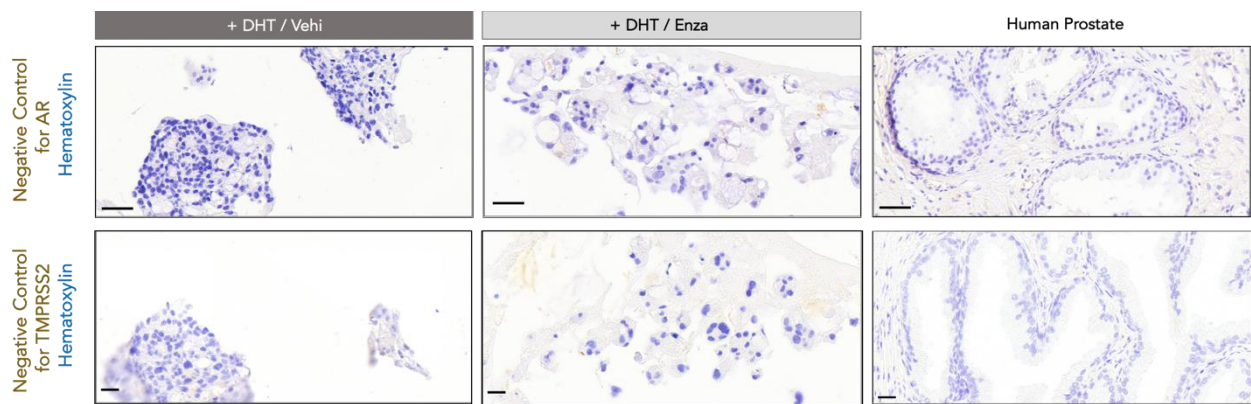


**Figure S6.** Isotype control of IHC analysis of AR and TMPRSS2 expression in PCSD1 organoids. Representative digital microscope images are shown of IHC isotype control of AR and TMPRSS2 IHC staining performed on 4% paraformaldehyde fixed, paraffin embedded 5  $\mu\text{m}$ . sections.

**Basal (CK5) and Luminal (CK8) Epithelial Cell Markers**

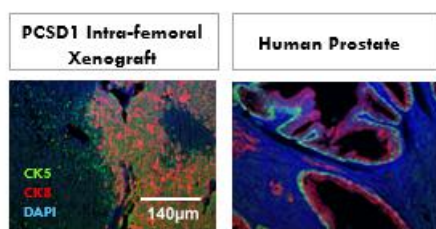


**Figure S7.**

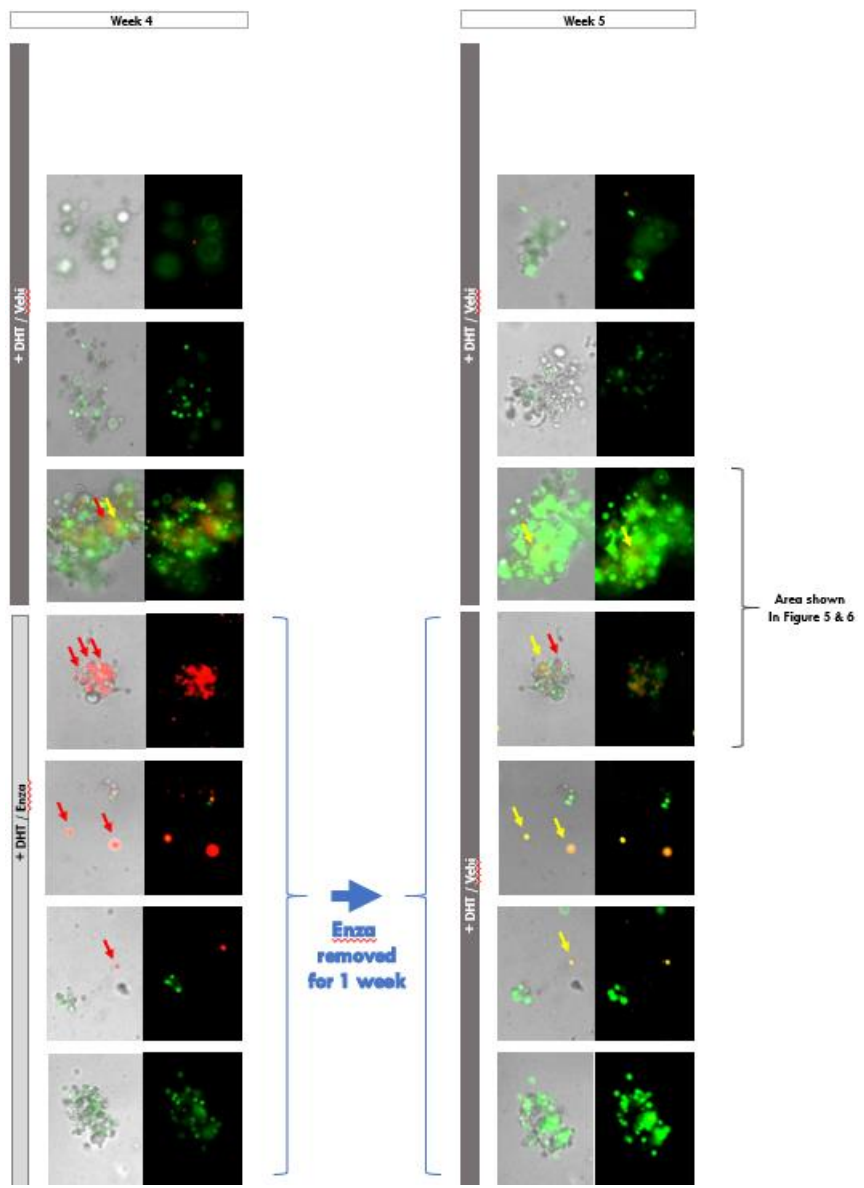


Figure S8.

**Table S1. Androgen Pathway Directed Therapy (APDT) Response Genes.** Full list of genes determined by Transcriptomics to be significantly up- and down-regulated in response to APDT is shown.

787 ADT RESPONSE GENES														
# Genes	269					518								
Direction	UP					DOWN								
RPKM	LOW					LOW					HIGH			
# Genes	98					171					206			
VILL	DCBLD1	NEURL3	APPL2	FOXO3	EXTL1	DHX58	LOC1005056	NUDT10	IRF7	IFIH1	KIF2C	ORC6		
BCAT1	ZEB1-AS1	DHRS9	MTSS1	FAM129A	SULT1B1	ABCD1	ADAP1	CUX2	SKA2	C19orf48	ABC6	SLC36A1		
FAM113B	SEMA3E	PLA2G2F	WDR72	CBLB	CORT	HMG83	C15orf42	DAPL1	VSTM2L	ERAP2	TRIM21	TAOK3		
O3FAR1	C14orf128	LIPG	LOC1004994	SOX13	HIST1H2BM	WDR76	CTSO	DOCK8	PDE9A	SAMHD1	MXD3	RGS11		
ABCA1	HSF4	MGLL	AR	PCK2	CXCL11	ARTN	SPTB	IFIT3	PKP1	NR4A1	CRIP2	PARP9		
SHISA2	EP400NL	ZNF365	RASSF5	IL36RN	WNT3	LOC143666	RTET1	IFIT1	KREMEN2	TCF19	GAMT	SLC10A7		
NCRNA00222	SERPINB7	TSPAN1	SH3BP5	SOX9	C9orf66	CD163L1	FBLN7	RSAD2	CCK	LOC400043	METTL7A	BEND4		
ZNF534	C1QTNF3	UGT1A1	FER1L4	ATP13A3	ABCC2	ESPL1	DSC3	CACNG4	TMSB15A	CITE04	THOP1	ASRGL1		
MECOM	GCET2	SLC5A1	PLA2G4F	ATP881	PSMB8	GNN	ACTR3B5P	BST2	HMG82	TBC1D8	BUB1B	HIST2H2BE		
CA12	LNX1	NBPF7	EXPH5	BAMB1	HIST1H4G	KIT	RAB9B	ZNF385B	FAM83D	COL6A1	KCNH2	NTAN1		
BHLHE41	BCAR3	FAM131B	SEMASA5	EPHA1	MNS1	DHFR	PHF11	IFI4L	RM12	NFYB	ARRB1	KCTD3		
PROX1	POGLUT1	MUC2	FAM13A	CAT	SPSB4	ADORA1	OSPLB1A	MX1	CKB	PANX2	ENDOG	PALM		
RGS16	TIMP4	C10orf10	PIM1	AN06	ALPK2	FAM189A2	TCP11L1	SCARA3	MELK	LPGAT1	NPEPL1	KDM4B		
FAM189A1	GRAMD3	PLA2G2A	THR8	PPARG	ANKRD1	BEGAIN	MTBP	FKBPS	RRM2	TACC3	SFXN5	AMOT		
PTPRE	FAM177B	CDKN2B	EGLN3	NFKBIZ	TRIM22	CIT	DUOX1	OAS2	ELOVL5	DDX60	STXBPS	FAM20C		
LOXL1	IRAK2	ZBTB7C	C20orf54	PCDH1	CTTNA2	DNAH9	LOC147804	GNMT	SORD	E2F2	DNLZ	TMEM26		
TNFSF8	NTF3	SDR16C5	PLEK2	GATA2	KCNMA1	TTC39C	WAS	GABARAPL1	C1QTNF6	CPE	ECI2	TRIM3		
DIRAS2	MAN1A1	COL5A2	CYP3A5	OSBP10	IRX3	PIGK	ARSI	MALT1	DTL	PTPN21	C21orf58	C9orf80		
OPN3	ZNF860	XYLT1	TNFSF15	PLCD3	GPER	PLK4	PAIP2B	IFITM1	SOAT1	UNKL	SKA3	GTf3A		
LPAR6	LX1L	HMGC52	POF1B	TNFRSF21	NTF4	LOX	FU37201	SP110	CDC20	ANKH	PRKAG2	NRGN		
ENG	GPR98	MMP28	VLDLR	GNIG12	CEP128	KIAA1377	MM52L	FSTL1	CAMK2B	STEAP4	ZNF615	SMYD2		
RASAL1	NGEF	CAPN8	RHBDL2	ABLM1	KCNH1	TMEM55A	KIAA1143	CMPK2	CROT	C16orf59	HIST1H2BH	FAM134B		
ADORA2B	EEDP1	SYTL2	TRPV6	TMEM154	FBXO15	XRCC2	ZNF354A	BIRC5	HJURP	DPP4	MSI1	ZNF238		
PLA2G4C	PPIP5K1	POLB	OSMR	ATP2B1	C2orf55	RAD51AP1	WDR93	ISG15	MKI67	ZNF613	SLC25A33	GMPR		
IKZF3	FMLN2L	LSAMP	CALN1	SLC12A2	CD200R1	BCRP3	STX2	UBE2L6	DX5X8	MOA0	CTS2	IAH1		
ITGB6	MSX2	DTX4	KIAA1211	PPP1R3B	C11orf53	LRRK1	DDHD2	REEP2	NKKX3-1	LOC389831	NEIL2	ISYNA1		
RNF152	C17orf109	REG4	PAK1	CD42EP2	ZSCAN12	LOC728723	TLK2	KLK3	PRIC285	HERC3	KIF20A	GINS2		
HSPG2	GPK2	ACSL5	BIOD1	OR56A3	NUDT13	LOXL2	HOXB13-AS1	UBE2C	POC1A	RTN1	MAPK12			
CDC89	SYTL5	CABLES1	CYP39A1	PDDZ2	LRFN2	MRS2P2	PARP10	GALNT14	NEK2	MCM10				
WNT4	TNFAIP2	OAF	UBA7	U7A8	C3orf33	LOC644714	C5orf39	RASD1	CLGN	NUDT1				
ZNF573	APCDD1	PLCD1	UGT2B10	ZNF578	CENPI	ANKRD34B	AURKA	OAS3	RAB28					
RNF207	KCNK5	KDELR3	FLG	NR3C1	LCAS	SMOC1	CCNB1	CDK1	MRPL23					
ALDH3B1	ACER2	PIP	CLDN8	SASS6	SLC45A1	GP2	TYMS	ZNF367	JAG2					
CCZ1	TSPAN8	SLFN5	GUCY2D	FANCD2	ADAMTS1	LAMP3	KIF11	DISP1	IF127					
FBXL13	LFNG	NIPAL1	KIAA1324	CDC7	LOC81691	MLLT11	MBOAT2	PPP3CA	TONSL					
PTPRN2	VCAN	ENPP5	ZNF114	PARD6B	DDB2	TNC	HMGCS1	PLEKHO1	HERC6					
ARHGAP24	BTG2	ERV3-1	JAZF1	GPR156	WDR66	GLRX	ENDOD1	NCAPG2	TSPAN33					
PLXNA2	C9orf150	HD38B1	MYO16	ZNF684	NPNT1	PXDN	BRCA1	FAM101B	RNASEH2A					
KCNIP3	GPR110	ABCC3	TMEM91	ACBD7	NT5M	CEP55	H2AFX	LEPREL1	PIK3AP1					
DENN2D	SPNS2	ITGA2	VWA5B2	C14orf176	VRK1	MAP2	PART1	EPN1	RNF145					
FOXO1	EPHB6	DUSP5	RARB	AKT3	REC8	HOMER2	NUF2	NRARP	CDKN2D					
RAPGEFL1	EEF1A2	ENTPD3	OSCAR	CCDC50	ZKBD	PMEPA1	TMEM150C	RILPL2	PTTG3P					
SLC5A7	LAD1	ZG16B	CTXN3	LOC338739	TMEM61	TOP2A	TPD52	CENPW	C9orf140					
ARNTL2	PTGS2	LRRN1	GYG2P1	FBXO27	PRKAR2B	PPP2R2C	PDLIM5	TMPPRSS2	CDC25A					
PP4R4L1	IL1RN	BCAS1	NKX3-2	PCGF5	GNCNT2	STMN1	C17orf76	IFI27L1	CCNA2					
ITPR1	CDH26	EDEM1	KCNK13	CHRM4	TL1L11	KLK1	PARP14	NELF						
SLC6A9	KCNN4	LAMC2	SNX24	FANCM	TIFA	ARHGAP11A	ZNF331	IMPA2	TFAP2C					
STK10	ARHGAP26	SRGAP3	SLTRK5	PER1	KLHL25	CDCA5	ZWINT	CCDC109B	AIFM2					
FSIP2	DUSP6	ST6GAL1	TMPPR59	RECK	LOC401093	CALD1	KLF9	FLJ20201	CENPL					
ID2B	CAMK2N1	LTBP1	ATOH8	NUMBL	MILP1	MAPK4	PLSCR1	FAM55C	FAM64A					
AHNAK2	KIAA1462	NPAS2	SAMD14	FAM54A	C5orf34	LOC729178	ATAD2	ZNF618	LRG1					
XYLB	TMC5	RAP1GAP	AKR1B1	GSG2	RAD51	IFI6	PLK1	STAT1	SMS					
TGF83	DGAT2	PLS1	CHD5	RBL1	CDADC1	IQGAP2	CDC43	TGFBR1	NAAA					
MICALCL	LY6D	ELF3	C18orf2	LMTK3	FAM160B1	MZT2A	KIFC1	ERCC6L	NEURL1B					
SATB1	FRY	TMEM51	APLP1	FRA10A/C1	GLIS2	E2F1	ANKS3	NCAPH2	PARVB					
FOXO3B	RGS2	EGFR	TTC32	C3orf58	SP5B1	HIST1H2AI	RFC3	IRF9	KIAA1324L					
B3GNT9	ROBO1	ADM2	TMCC3	C1QL1	NCRNA0008	ZNF614	ASF1B	FBXO5	MIIP					
C17orf57	APLN	SYT1	AASS	KIF4A	THAP10	FAM43A	ANLN	FANCI	CCDC34					
COL16A1	PCDH20	LOC149134	MLK7-AS1	PCYT1B	ACE2	SECTM1	PEX10	UBE2D1	KIAA0889					
RFX3	ITGB4	LOC100289255	CIB3	C7orf13	TRAFF3IP2-A5	PRC1	AGPAT2	LBH	ZNF761					
SH3RF3	SUSD4	UGCG	SP100	FAM71E1	TAPT1	TPX2	PKMYT1	GINS1	FANCG					
FAM86C1	DAPK1	DHR53	BRIP1	D2IP1	LOC1001282	CPM	PM20D2	FSCN1	C9orf91					
AGPAT4	OVGP1	NTN4	CDT1	MLF1IP	B3GNT4	DDX60L	FAM149A	RAP2A	TRIM36					
43893	CNGA1	LM04	SRSF12	C9orf21	SPRYD7	ELOV4	PTT1	ACOT7	UBE2E3					
ALPK3	HK2	SERPINI1	USP18	C4orf21		PBK	PRDX6	RAMP1	RECQL4					
LOC100287616	RCAN2	NRP1	GLTPD2	SRDS1A/P1		BRP44	TRIP13	UBE2T	SMC2					
COL3A1	TMPPR54	NIPAL2	LOC389676	LOC100128822		NPNT	TNFSF12,TNFSF12,TNFSF12	EGFL7	VWA1					
P4HA3	ZYX	ETV4	ERAS	ZNF813		C19orf79	IFI44	CDCA8	MAPK8IP2					
MATN2	SCIN	TMEM117	DISC1	NCRNA00294		WTIP	GYG2	AURKB	WDR34					
GEMIN8P4	SPRY2	GALE	CDC45	C9orf167		CBR3	ANGPT2	MCM5	CHTF18					
CES4A	TCP11L2	DISP2	DIAPH3	NXT2		FOXM1	TP53TG1	KLK4	TTY15					

Interferon Signaling					Cell Cycle					Circadian Clock				
UP		DOWN		NC HIGH RPKM	UP		DOWN		NC HIGH RPKM	UP		DOWN		NC HIGH RPKM
18		0		64	127		109		1535	15		198		85
18	0	40	24		18	109	984	551		7	8	113	85	
BST2	(none)	ABCE1	DCST1		APPL2	AKT3	AAAS	ABC81		ARNTL2	ADORA1	AHCY	AANAT	
IFI27		ADAR	HLA-F		BCAT1	ANLN	AATF	ACD		BHLHE41	CDK1	ATF2	ADA	
IFI6		CDC37	HLA-G		BTG2	AURKA	ABL1	ADAM17		EGFR	KLF9	ATF4	ADCY1	
IFIT1		CNOT7	HLA-H		CABLES1	AURKB	ACTB	AFAP1L2		NPAS2	NR3C1	ATF5	ADPOQ	
IFIT3		FADD	IFI35		CAMK2N1	BIRC5	ACTR10	AHCTF1		OPN3	PER1	BHLHE40	ADORA1	
IFITM1		HLA-A	IFITM2		CDKN2B	BRCA1	ACTR1A	AKT3		PPARG	SPSB4	BTBD9	ADORA2A	
IRF7		HLA-C	IFNA1		EGFR	BRIP1	ACTR1B	ALMS1		PROX1	TOP2A	BTRC	AGRP	
IRF9		HLA-E	IFNA5		LFNG	BUB1B	ACTR2	ALOX15B		TYMS		CARM1	ARNTL	
ISG15		HSP90AB1	IFNB1		MECOM	CCNA2	ACTR3	ANAPC1				CDK4	ARNTL2	
MX1		IFNAR1	IKBKE		MSX2	CCNB1	ACTR8	ANAPC4				CHEK1	ASS1	
OAS2		IFNAR2	IRF1		PIM1	CDC20	ACVR1	ANKK1				CLDN4	ATG7	
OAS3		IP6K2	IRF4		PROX1	CDC25A	ACVR1B	ANKRD31				CLOCK	ATOH7	
PSMB8		IRAK1	IRF5		PTGS2	CDC45	ADAMTS1	ANKRD53				CPT1A	ATR	
RSA2		IRF2	ISG20		RGS2	CDC7	ADARB1	APAF1				CREB1	BHLHE41	
SAMHD1		IRF3	MMP12		SOX9	CDC43	AKAP8	APP				CREBBP	CARTPT	
SP100		IRF6	NLRCS		SPRY2	CDC45	AKAP8L	ARHGEF10				CREM	CHD9	
STAT1		JAK1	PSMB8		STK10	CDCA8	AKAP9	ARHGEF2				CRTC2	CHRN8B	
USP18		LSM14A	SOCS1		WNT4	CDK1	AKT1	ARID3A				CRTC3	CRTC1	
		MAVS	SOCS3			CDKN2D	AKT2	ARNTL				CRY1	DDC	
		METTL3	SP100			CDT1	ALKB4	ASAH2				CRY2	DRD2	
		MUL1	TRIM6			CENPI	ANAPC10	ASPM				CSNK1D	DRD4	
		MX2	USP18			CENPL	ANAPC11	ASZ1				CSNK1E	EGR3	
		MYD88	XAF1			CENPW	ANAPC13	ATAD5				CUL1	EZH2	
		OAS1	ZBP1			CEP55	ANAPC16	ATM				DDB1	F7	
		PTPN1				CHTF18	ANAPC2	ATP2B4				DYRK1A	GHRHR	
		PTPN11				CIT	ANAPC5	ATR				EP300	GHRL	
		PTPN2				DHFR	ANAPC7	ATRIP				FBXL3	GPR157	
		PTPN6				DTL	ANGEL2	ATRX				FBXW11	GPR176	
		SETD2				E2F1	ANK3	AURKC				FBXW7	HCRTR2	
		SHMT2				E2F2	ANKLE2	AXIN2				GFP1	HNF1B	
		STAT2				ERCC6L	ANKRD17	B9D2				GNA11	HNF4A	
		TBK1				ESPL1	ANXA11	BAK1				GNAQ	HS3ST2	
		TREX1				FAM83D	APBB2	BANP				GSK3B	KCNA2	
		TRIM56				FANCD2	APC	BCAT1				HDAC1	KCN8D2	
		TTL12				FANCI	APEX1	BCL2				HDAC2	KLF15	
		TYK2				FANCM	APEX2	BIN1				HDAC3	LEP	
		UBE2K				FBXO5	APPL1	BLM				HEBP1	MAGE62	
		WNT5A				FOXM1	ARAP1	BMP4				HIF1A	MC3R	
		YTHDF2				GINS1	ARF1	BMP7				HNRNPD	MEF2C	
		YTHDF3				GINS2	ARF6	BOLL				HNRNPL	MTNR1A	
						HJURP	ARL3	BOP1				HNRNPR	MTNR1B	
						KIF11	ARL8A	BORA				HNRNPU	NGFR	
						KIF20A	ARL8B	BRCA2				HUWE1	NKX2-1	
						KIF2C	ARPP19	BRD7				ID1	NLG1	
						KIF4A	ASNS	BRIP1				ID3	NMU	
						KIFC1	ATF2	BTBD18				ID4	NOS2	
						MAPK12	ATF5	BTC				IMPDH2	NPY2R	
						MAPK4	AURKAIP1	BTG3				JUN	NR0B2	
						MCM10	AVP1	BTG4				JUND	NR1D1	
						MCM5	AZI2	BTN2A2				KDM2A	NR1H3	
						MELK	BABAM1	BUB1				KDMSA	NTRK2	
						MIIP	BACH1	C10orf90				KLF10	NTRK3	
						MKI67	BAG6	C14orf39				MAGED1	OPN3	
						MNS1	BANF1	CAMK2A				MAPK10	OPRL1	
						MTBP	BAP1	CAPN3				MAPK8	PER1	
						MYO16	BAX	CAV2				MAPK9	PER2	

Prostate Stem/Progenitor				Cell Cycle				Circadian Clock			
UP	DOWN	NC HIGH RPKM	NC LOW RPKM	UP	DOWN	NC HIGH RPKM	NC LOW RPKM	UP	DOWN	NC HIGH RPKM	NC LOW RPKM
8		58		127		1535		15		198	
5	3	22	36	18	109	984	551	7	8	113	85
AR	BIRC5	BMI1	ALDH1A2	MZT2A	BBS4	CC2D1B				MED1	PER3
ETV4	DPP4	CARM1	ALDH8A1	NCAPG2	BCCIP	CCDC155				MEF2D	PIWIL2
ITGA2	GPER	CDH1	ATXN1	NCAPH2	BCL2L1	CCDC36				METTL3	PML
PLA2G2A		CTNNB1	BCL2	NEK2	BCL2L11	CCDC69				MTOR	PPARA
SOX9		FOXA1	BMP4	NKX3-1	BCL6	CCDC8				MYBBP1A	PPIRG1A
		HOXA13	BMP7	NR3C1	BCR	CCNA1				MYCBP2	PRKAA2
		ID4	CA9	NR4A1	BECN1	CCNB3				NAGLU	PROK1
		ITGA6	CD38	NUF2	BEX2	CCND2				NAMPT	PTEN
		KRT15	CD74	ORC6	BID	CCNE1				NCOA1	ROCK2
		KRT18	DLK1	PARD6A	BIN3	CCNI2				NCOA2	RORA
		KRT19	EGF	PBK	BIRC2	CCNLJ				NCOA6	RORB
		KRT7	ETS1	PKMYT1	BIRC6	CCNT2				NCOR1	RORC
		LIFR	ETV1	PLK1	BLCAP	CD28				NDUFA9	RPE65
		MYC	FGFR2	PLK4	BLZF1	CDC14A				NFIL3	SERpine1
		NFE2L2	FGFR3	PNPT1	BMI1	CDC14B				NONO	SIX3
		RB1	IGF1	POC1A	BOD1	CDC14C				NR1D2	SLC6A4
		SIRT1	IGF2	PPP2R2C	BRCC3	CDC25C				NR2F6	SMARCD3
		SOX4	KRT13	PPP3CA	BRD4	CDC45				NRIP1	SPSB4
		SP1	KRT4	PRC1	BTG1	CDC7				OGT	SRD5A1
		STAT3	KRT6A	PRKAG2	BTTC	CDC2A				PHLPP1	STAR
		TACSTD2	LIF	PRKAR2B	BUB3	CDH13				PPP1CA	TGS1
		WNT5A	MSLN	PSMB8	C11orf80	CDK11A				PPP1CB	TH
			NES	PTTG1	C2CD3	CDK11B				PPP1CC	TNFRSF11A
			NRG2	PTTG3P	C6orf89	CDK18				PRKAA1	TP53
			PIGR	RAD51	CAB39	CDK7				PRKDC	TPH1
			POU5F1	RBL1	CABLES2	CDKL1				PRMT5	TPH2
			PTEN	REC8	CALM1	CDKL2				PSPC1	USP2
			RSP03	RFC3	CALM2	CDKL3				RAI1	USP46
			SNAI1	RMI2	CALM3	CDKL4				RBM4	ZFHX3
			SNAI2	RRM2	CALR	CDKN1C				RBM4B	
			TGFB1	RTEL1	CARM1	CDT1				RELB	
			TNFRSF1B	SASS6	CASP2	CECR2				RPS27A	
			TP63	SKA2	CASP3	CENPA				RXRA	
			TWIST1	SKA3	CASP8AP2	CENPE				SETX	
			VEGFC	SLC25A33	CBX3	CENPI				SFPQ	
			WNT10B	SMC2	CBX5	CENPJ				SIAH2	
				STMN1	CCAR1	CENPK				SIK1	
				TACC3	CCDC124	CENPN				SIN3A	
				TAOK3	CCNB1IP1	CENPP				SIRT1	
				TGFBR1	CCNB2	CENPQ				SKP1	
				TLK2	CCNC	CENPT				SREBF1	
				TOP2A	CCND1	CEP120				SRRD	
				TPX2	CCND3	CEP135				SUV39H1	
				TRIM21	CCND8P1	CEP152				SUV39H2	
				TRIM36	CCNE2	CEP192				TARDBP	
				TRIP13	CCNF	CEP290				TBL1X	
				TYMS	CCNG1	CEP63				TBL1XR1	
				UBE2C	CCNG2	CEP70				THRAP3	
				UBE2D1	CCNH	CEP72				TIMELESS	
				VRK1	CCNI	CEP76				TOP1	
				WDR76	CCNJ	CEP97				UBA52	
				XRCC2	CCNK	CHEK2				UBB	
				ZWINT	CCNL1	CHORDC1				UBC	
					CCNL2	CIT				UBE3A	
					CCNO	CKS1B				USP7	
					CCNT1	CLSPN				USP9X	
					CCNY	CLTCL1				WDR5	

NEPC/Neurogenic				Cell Cycle				Neurogenesis			
UP	DOWN	NC HIGH RPKM	NC LOW RPKM	UP	DOWN	NC HIGH RPKM	NC LOW RPKM	UP	DOWN	NC HIGH RPKM	NC LOW RPKM
20		180		127		1535		81		1314	
6	14	85	95	18	109	984	551	41	40	630	684
AR	AURKA	ABCC4	ADAM7		CCNYL1	CNOT6L		ABLIM1	ANKRD1	ABC42	ABLIM2
GATA2	AURKB	ACSL3	ASCL3		CCP110	CNTD1		APCDD1	ARTN	ABI1	ACSL4
GPX2	C1orf116	AMACR	ASXL3		CCPG1	CNTD2		APPL2	ATOH8	ABI2	ACTBL2
ITGA2	E2F1	ARHGAP8	CAND2		CD2AP	CNTLN		ATP8B1	AURKA	ABL1	ADAM22
PROX1	FKBP5	CAMKK2	CATSPERB		CDC123	CNTRL		BHLHE41	C1QL1	ABL2	ADCY1
SOX9	FOXM1	CCND1	CDH2		CDC16	CNTROB		BTG2	CAMK2B	ABT1	ADORA2A
	GNMT	CCND3	CDX2		CDC23	CROCC		COL3A1	CCK	ACAP3	ADRA2B
	KLF9	CDH1	CENPN		CDC25B	CSNK2A2		EGFR	CDC20	ACSL3	ADRA2C
	KLK3	CDK4	CHGA		CDC26	CSPP1		EPHA1	CDK1	ACTB	AGBL4
	KLK4	CREB1	CIITA		CDC27	CTC1		EPHB6	CHD5	ACTR2	AGER
	NKK3-1	CREB3	CREB5		CDC34	CUZD1		FOXO3	CIT	ADAM10	AGT
	NR3C1	CREB3L1	CYLD		CDC37	CXCR5		FRY	CTNNA2	ADARB1	AKNA
	PMEPA1	CREB3L2	ESR1		CDC42	CYLD		GATA2	CTS2	ADCY6	ALDH1A2
	TMPRSS2	CREBBP	ESR2		CDC5L	CYP26B1		LAMC2	CUX2	ADM	ALK
		CREBL2	ETV5		CDC6	CYP27B1		LMO4	DHFR	ADNP	AMIGO1
		CSD61	EZH2		CDC73	DACH1		MATN2	DISC1	ADNP2	ANKRD1
		CTBP2	FHIT		CDK10	DACT1		NGEF	E2F1	AFG3L2	APOA1
		DICER1	FOXA2		CDK12	DBF4		NRP1	HMGB2	AGRN	APOD
		DNMT1	FOXB1		CDK13	DBF4B		NTF3	IRX3	AGTPBP1	APOE
		EFNA4	FOXC1		CDK14	DCC1		NTN4	JAG2	AHI1	APP
		ELL2	FOXP2		CDK16	DCLRE1B		PAK1	KIT	AKT1	ARC
		ENO2	GATA1		CDK17	DCUN1D3		PLXNA2	MAP2	AKT2	ARHGAP33
		EPCAM	GATA4		CDK19	DDX11		PPARG	MAPK8IP2	ALCAM	ARHGAP4
		EPN3	GLI1		CDK2	DDX4		PROX1	MYO16	ALKBH1	ARHGEF10
		ERBB3	GLI2		CDK20	DIFR		RAP1GAP	NTF4	ALS2	ARHGEF2
		EVPL	GLI3		CDK2AP1	DIRAS3		RASAL1	NUMBL	ANAPC2	ARNTL
		FOLH1	HES2		CDK2AP2	DIS3L2		RGS2	PDLIM5	ANK3	ARSB
		FOXA1	HES7		CDK3	DLGAP5		ROBO1	PPP3CA	ANKRD27	ARTN
		FOXG1	HESX1		CDK4	DMC1		SEMA3E	RAP2A	ANKS1A	ARX
		FOXP1	HEY1		CDK5	DMRT1		SEMAS5A	RARB	AP2A1	ASPM
		GSTP1	HOXA1		CDK5R1	DNA2		SERPIN1I	SAMD14	APBB2	ASTN1
		HERPUD1	HOXA5		CDK5RAP1	DNMT3L		SOX13	SLTRK5	ARF1	ATCAY
		HES6	HOXB2		CDK5RAP2	DRD2		SOX9	SPTB	ARF4	ATOH1
		HIF1A	HOXB3		CDK5RAP3	DUSP13		SRGAP3	STMN1	ARF6	ATOH7
		HOXA10	HOXB4		CDK8	DYNC1I1		SYT1	TAOK3	ARFGEF1	ATOH8
		HOXA11	HOXB6		CDK9	DYNC1I2		THR8	TGFBR1	ARHGAP35	ATP1B2
		HOXA13	HOXB7		CDKL5	DYRK3		TNFRSF21	TNC	ARHGAP44	ATP2B2
		HOXA9	HOXC10		CDKN1A	E2F6		UGCG	VSTM2L	ARHGDIA	ATP7A
		ID1	HOXC4		CDKN1B	E2F7		VLDLR	WNT3	ARHGEF12	ATP8A2
		ID3	HOXC5		CDKN3	E2F8		WNT4	XRCC2	ARID1B	AUTS2
		ID4	HOXC6		CEBPA	EFHC1		ZNF365	ARL3	AVIL	
		ITGA6	HOXC9		CENPM	EGF			ASAP1	AXL	
		ITGB1	HOXD1		CENPO	EPGN			ASTN2	AZU1	
		JUN	HOXD3		CENPV	ERCC4			ATAT1	B4GALT6	
		KLF10	HOXD4		CEP164	ERCC6			ATF1	BARHL1	
		KLF13	HOXD8		CEP250	EREG			ATF4	BCHE	
		KLF16	HOXD9		CEP57	ERN1			ATF5	BCL11A	
		KLF3	INSM1		CEP68	ESCO2			ATL1	BCL11B	
		KLF5	KCND2		CEP78	ESPL1			ATXN10	BCL2	
		KLF6	KIAA0408		CEP85	ESRRB			B2M	BDNF	
		KLF7	KLF1		CETN2	ETAA1			B3GNT2	BEND6	
		KLK2	KLF12		CETN3	EV12B			B4GALT5	BHLHA15	
		KRT18	KLF14		CFL1	EV15			BACE2	BHLH89	
		KRT19	KLF15		CGREF1	EXD1			BAG5	BHLHE41	
		LEF1	KLF17		CGRRF1	EXO1			BAIAP2	BIN1	
		MAPKAPK3	KLF2		CHAF1A	EZH2			BAX	BLK	
		MYC	KLF8		CHD3	FAM107A			BBS4	BMP4	

NEPC/Neurogenic				Cell Cycle				Neurogenesis			
UP	DOWN	NC HIGH RPKM	NC LOW RPKM	UP	DOWN	NC HIGH RPKM	NC LOW RPKM	UP	DOWN	NC HIGH RPKM	NC LOW RPKM
20		180		127		1535		81		1314	
6	14	85	95	18	109	984	551	41	40	630	684
MYH9	LHX2	CHEK1	FAM9A	BCL6	BMP5						
NR3C2	LHX3	CHFR	FANCA	BHLHE40	BMP7						
NUP93	LHX4	CHMP1A	FANCD2	BLOC1S1	BMPR1A						
OPHN1	LHX5	CHMP1B	FANCM	BLOC1S2	BMPR2						
PARP1	LHX6	CHMP2A	FAP	BLOC1S3	BOC						
PPAP2A	LMAN1L	CHMP2B	FBXL22	BMP6	BTBD8						
PRKDC	LRRC16B	CHMP4A	FBXL7	BMPR1B	BTG4						
PRRS	MMP2	CHMP4B	FBXL8	BNIP3	C1QL1						
PSMA1	MYT1	CHMP4C	FBXO31	BOK	C21orf91						
RB1	NCAM1	CHMP5	FBXO4	BSG	C3						
RBBP6	NKX2-1	CHMP6	FBXO43	BTBD1	CSAR1						
RBPJ	NKX2-2	CHMP7	FEM1B	BTBD2	C8orf37						
REST	ONECUT1	CHTF8	FER	BTBD3	CABP4						
RGS10	ONECUT2	CIB1	FES	BTBD6	CAMK1D						
RIPK2	ONECUT3	CINP	FGF8	C12orf57	CAMK2A						
SEC11C	PAX5	CITED2	FGFR1	C9orf72	CCDC88A						
SIX1	PAX8	CKAP2	FGFR2	CALR	CCKAR						
SLC25A37	PCSK1	CKAP5	FHL1	CAMK2G	CD38						
SLC44A4	PGR	CKS2	FIGN	CAMSAP1	CDH2						
SOX4	POU2F1	CLASP1	FKBP6	CAPRIN1	CDH23						
SPDEF	POU3F1	CLASP2	FLT3LG	CAPRIN2	CDH4						
STEAP1	POU3F2	CLIC1	FMN2	CARM1	CDHR1						
STEAP2	POU5F1	CLIP1	FOSL1	CASP3	CDKL3						
SUZ12	SCGN	CLOCK	FOXC1	CASZ1	CDNF						
TACSTD2	SEZ6	CLTA	FOXE3	CBFA2T2	CDON						
TC2N	SNAI1	CLTC	FOXN3	CD9	CELSR1						
TCF12	SNAI2	CNOT1	FSD1	CDC42	CELSR3						
TRIM33	SPINK1	CNOT10	FZD3	CDH1	CEND1						
	SYP	CNOT2	FZD9	CDK16	CEP120						
	SYT11	CNOT3	GAS1	CDK5	CEP290						
	TP53	CNOT4	GAS2	CDK5R1	CHD5						
	TP63	CNOT6	GAS6	CDK5RAP1	CHD7						
	TRIM9	CNOT7	GDPD5	CDK5RAP2	CHL1						
	TWIST1	CNOT8	GEM	CDK5RAP3	CHN1						
	UPK2	CNPPD1	GEN1	CDKL5	CHDL						
	ZBTB46	COPS5	GFI1	CEPB8	CHRM1						
	ZEB1	CRADD	GINS3	CELSR2	CHRNA3						
	ZEB2	CREBL2	GINS4	CERS2	CHRN8B						
		CRLF3	GJA1	CFL1	CIT						
		CRY1	GJC2	CFL2	CLU						
		CSNK1A1	GLI1	CFLAR	CNR1						
		CSNK1D	GPNMB	CI1	CNTF						
		CSNK1E	GPR3	CLCF1	CNTN2						
		CSNK2A1	GRK5	CLMN	CNTN4						
		CSNK2B	HACE1	CLN5	CNTN6						
		CTBP1	HAUS1	CNP	CNTNAP1						
		CTCF	HAUS3	CNTF	CNTNAP2						
		CTDNEP1	HAUSS	COBL	COL3A1						
		CTDP1	HAU6	COPS2	CPEB3						
		CTDSP1	HAU7	CPNE1	RBM1CPNE5						
		CTDSP2	HECW2	CREB1	CPNE9						
		CTDSPL	HELLS	CREB3L2	CRABP2						
		CTNNB1	HEPACAM2	CRK	CRB1						
		CUL1	HERC2	CRKL	CRMP1						
		CUL2	HFM1	CSK	CRTAC1						
		CUL3	HHEX	CSNK1D	CRTC1						
		CUL4A	HLA-G	CSNK1E	CSF1						

Axon Guidance				Cell Cycle				Neurogenesis			
UP	DOWN	NC HIGH RPKM	NC LOW RPKM	UP	DOWN	NC HIGH RPKM	NC LOW RPKM	UP	DOWN	NC HIGH RPKM	NC LOW RPKM
13		108		127		1535		81		1314	
12	1	51	57	18	109	984	551	41	40	630	684
ABLIM1	PPP3CA	ABL1	ABLIM2		CUL4B	HMGNS		CTDSP1	CSF1R		
EPHA1		ARHGEF12	CXCL12		CUL5	HORMAD1		CTNNA1	CSPM3		
EPHB6		CDC42	CXCR4		CUL7	HSPA2		CTNNB1	CSPG4		
NGEF		CDK5	DCC		CUL9	HUS1B		CTTN	CSPG5		
NRP1		CFL1	DPYSL2		CYP1A1	HYAL1		CUL4B	CTF1		
NTN4		CFL2	DPYSL5		DAB2IP	IFNW1		CUL7	CTHRC1		
PAK1		EFNA1	EFNB1		DAPK3	IGF1		CUX1	CTNNA2		
PLXNA2		EFNA3	EPHA3		DCLRE1A	IGF2		CYB5D2	CTNND2		
ROBO1		EFNA4	EPHA4		DCTN1	IKZF1		CYFIP1	CX3CR1		
SEMA3E		EPHA2	EPHAS		DCTN2	IL1A		DAB2IP	CXCL12		
SEMA5A		EPHB2	EPHA6		DCTN3	INCA1		DAG1	CXCR4		
SRGAP3		EPHB3	EPHA7		DDB1	INHA		DAGLB	DAAM2		
	GNA11	EPHA8			DDIT3	INHBA		DAPK3	DAB1		
	GNA12	EPHB1			DDRGK1	INO80		DBN1	DAGLA		
	GNA13	EPHB4			DDX39B	INSM1		DBNL	DCC		
	GSK3B	FES			DDX3X	INSM2		DDIT4	DCCD2		
	HRAS	FYN			DHCR24	IRF1		DDR1	DCHS1		
	ITGB1	L1CAM			DIDO1	ITGB3BP		DX56	DCLK1		
	KRAS	LRRC4C			DKC1	JAK2		DX6	DCLK2		
	LIMK1	MET			DLG1	KAT2B		DENND5A	DCT		
	LIMK2	NFAT5			DMTF1	KATNB1		DGUOK	DHFR		
	MAPK1	NFATC1			DNM2	KIAA1614		DHX36	DIO3		
	MAPK3	NFATC2			DNMT3A	KIF14		DICER1	DISC1		
	NCK1	NFATC4			DONSON	KIF15		DISC1	DIXDC1		
	NCK2	NGEF			DOT1L	KIF18A		DKK1	DLG4		
	NFATC3	NRAS			DRG1	KIF18B		DLG5	DLL1		
	PAK2	NTN1			DSCC1	KIF20B		DLX1	DLL3		
	PAK4	NTN3			DSN1	KIF23		DNM1L	DLL4		
	PAK6	PLXNA2			DUSP1	KIF25		DNM2	DLX2		
	PLXNA1	PLXNB3			DUSP3	KIF4A		DNMT3A	DLX5		
	PLXNA3	PLXNC1			DYNC1H1	KIF4B		DTNBP1	DNER		
	PLXNB1	PPP3CC			DYNC1LI1	KLHDC8B		DUSP10	DNM3		
	PLXNB2	PPP3R2			DYNC1LI2	KLHL13		DVL1	DNMT3B		
	PPP3CB	RAC2			DYNLL1	KLK10		DVL2	DOCK10		
	PPP3R1	RASA1			DYNLL2	KNTC1		DVL3	DOCK7		
	PTK2	RND1			DYNLT1	L3MBTL1		DYNL1	DOK1		
	RAC1	ROBO2			DYNLT3	LATS2		ECT2	DOK4		
	RAC3	ROBO3			DYRK1A	LEP		EED	DOK6		
	RGS3	ROCK2			E2F3	LIF		EEF2	DPSL2		
	RHOA	SEMA3A			E2F4	LIG1		EEF2K	DPSL5		
	RHOD	SEMA3C			E2F5	LIN37		EFNA1	DRD1		
	ROCK1	SEMA3D			E4F1	LIN54		EFNA3	DRD2		
	SEMA3B	SEMA3E			ECD	LIN9		EFNA4	DTX1		
	SEMA3F	SEMA3G			ECT2	LPIN3		EHD1	DUOXA1		
	SEMA4A	SEMA4F			EDN1	LSM11		EIF2AK4	DYNC2H1		
	SEMA4B	SEMA4G			EED	LZTS1		EIF2B1	EDNRB		
	SEMA4C	SEMA5B			EHMT1	MAD1L1		EIF2B2	EFHC2		
	SEMA4D	SEMA6B			EHMT2	MAEL		EIF2B3	EFHD1		
	SEMA6A	SEMA6C			EID1	MAGI2		EIF2B4	EFNB1		
	SLT1	SEMA6D			EIF2AK4	MAP3K8		EIF2B5	EGR2		
	SRGAP2	SEMA7A			EIF4E	MAPK15		EIF4E	EIF4ENIF1		
		SLT1			EIF4EBP1	MAPRE2		EIF4G1	ELL3		
		SLT2			EIF4G1	MARVELD1		EML1	ELP3		
		SLT3			EIF4G2	MCM8		ENAH	EMB		
		SRGAP1			EMD	MCPH1		ENC1	EMX1		
		UNC5A			EME1	MCTS1		EP300	EMX2		
		UNC5C			EME2	MDM1		EPHA2	EN2		

Home Response				Cell Cycle				Neurogenesis			
UP	DOWN	NC HIGH RPKM	NC LOW RPKM	UP	DOWN	NC HIGH RPKM	NC LOW RPKM	UP	DOWN	NC HIGH RPKM	NC LOW RPKM
29		398		127		1535		81		1314	
16	13	149	249	18	109	984	551	41	40	630	684
APLN	ABCC2	AACS	AANAT		EML1	MDM4				EPHB2	EOMES
C1QTNF3	ACE2	ABAT	ABCC2		EML4	MECOM				EPHB3	EPHA10
CYP3A5	ADORA1	ACAA1	ABCC8		ENSA	MEI1				ERBB2	EPHA3
DGAT2	AKR1B1	ADM	ACE		EP300	MICAL3				ERBB3	EPHA4
DHRS3	ARRB1	AIMP1	ACE2		EPB41	MIS18BP1				ERCC2	EPHA5
DHRS9	CPE	ALDH1A3	ACHE		EPB41L2	MLF1				ERCC3	EPHA6
EGFR	CTS2	ALDH9A1	ACSL4		EPC1	MLH3				ESRP1	EPHA7
HSD3B1	DPP4	ARL2	ACVR1C		EPS8	MLXIPL				ETV6	EPHA8
IL1RN	DUOX1	ARL2BP	ACVR2B		ERCC1	MND1				EXT1	EPHB1
ITPR1	NKX3-1	ARNT	ADCY5		ERCC2	MNS1				EZR	EPHB4
PTPRN2	PER1	ATP1A1	ADH1A		ERCC3	MOV10L1				FA2H	EPO
RFX3	PPP3CA	ATP6AP2	ADH1B		ERF	MRGPRX2				FARP1	ERBB4
SDR16C5	SULT1B1	BACE2	ADH1C		ERH	MSH3				FARP2	ERCC6
SLC5A7		BAD	ADH6		ESCO1	MSH4				FBXO38	ETV1
UGT1A1		BAIAP3	ADH7		EZR	MSTO1				FBXO45	ETV5
WNT4		BCAT2	ADIPOQ		FAM32A	MSX1				FBXO7	EVX1
		BMP6	ADORA1		FBXL12	MSX2				FBXW8	EYA1
		C2CD2L	ADRA2C		FBXL18	MTBP				FEZ2	EZH2
		CAMK2G	AGT		FBXL3	MYB				FGF13	F2
		CAPN10	AGTR1		FBXO6	MYBL1				FKBP4	FAIM
		CDK16	AKR1B1		FBXO7	MYO16				FLNA	FAIM2
		CLCN2	AKR1B10		FBXW11	MYOCD				FLOT1	FAT4
		CLOCK	AKR1B15		FBXW5	NAE1				FMR1	FBXO31
		COMT	AKR1C3		FBXW7	NANOS3				FOXA1	FES
		CPT1A	ALDH1A1		FEN1	NCAPG				FOXG1	FEV
		CREB1	ALDH1A2		FGFR1OP	NCAPH				FRS2	FEZ1
		CRY1	ALDH8A1		FIGNL1	NDC80				FUT9	FEZF1
		CRY2	ANO1		FKBPL	NEK1				FZD1	FGF5
		CYP1A1	APOA1		FLCN	NEK10				FZD4	FGF8
		CYP2R1	ARNTL		FLNA	NEK11				FZD5	FGFR1
		DGAT1	AWAT2		FOXA1	NEK3				GAB2	FGFR2
		DGKQ	BCO2		FOXG1	NEK9				GAK	FIG4
		DHCR7	BLK		FOXO4	NES				GBA2	FKBP1B
		DHRS11	BMP5		FZR1	NME7				GDF11	FLRT1
		ECE1	BMP8A		GADD45A	NOTCH1				GD11	FLRT2
		ECE2	C1QTNF1		GADD45B	NOX5				GIGYF2	FLRT3
		EDN1	C1QTNF3		GADD45G	NPAT				GNAI1	FN1
		ENSA	CACNA1C		GADD45GIP1NPM2					GNAI2	FOXA2
		ENY2	CACNA1D		GAK	NPR2				GNAI3	FOXB1
		FAM3B	CACNA1E		GAR1	NR2E1				GOLGA4	FOXD1
		FDX1	CACNA1H		GAS2L1	NR4A3				GORASP1	FOXN4
		FOXA1	CACNA2D2		GATA6	NSL1				GPC1	FRYL
		FURIN	CARTPT		GBF1	NUP107				GPC2	FSCN2
		FZD4	CASR		GIGYF2	NUP155				GRB10	FSTL4
		GHR	CCKAR		GIPC1	NUP35				GRB2	FYN
		GLUD1	CCL5		GIT1	OFD1				GRB7	FZD2
		GLUL	CD38		GMNN	ORC1				GRN	FZD3
		GNAS	CFTR		GNAI1	ORC4				GSK3A	FZD7
		HADH	CGA		GNAI2	PARD3B				GSK3B	FZD8
		HIF1A	CHD7		GNAI3	PARD6A				GSTP1	FZD9
		HMGCR	CHST8		GOLGA2	PARD6B				HDAC1	GAB1
		HMGN3	CHST9		GORASP1	PARD6G				HDAC11	GABRA5
		HPN	CMA1		GORASP2	PARP3				HDAC2	GALR2
		HSD17B11	CNR1		GSK3B	PAX6				HDAC5	GAS6
		HSD17B12	COLQ		GSPT1	PCGF2				HDAC6	GAS7
		HSD17B4	CORIN		GTF2H1	PCGF6				HES6	GBX1
		ICA1	CPLX1		GTPBP4	PDE3A				HEXB	GBX2

Home Response				Cell Cycle				Neurogenesis				
UP	DOWN	NC HIGH RPKM	NC LOW RPKM	UP	DOWN	NC HIGH RPKM	NC LOW RPKM	UP	DOWN	NC HIGH RPKM	NC LOW RPKM	
29		398			127	1535			81	1314		
16	13	149	249	18	109	984	551	41	40	630	684	
IDE	CPLX3	HAUS2	PDGFB	HIF1A	GCM1							
ILDR1	CRABP1	HAUS4	PDGFRB	HIPK1	GCM2							
IRS2	CRABP2	HAUS8	PER2	HIPK2	GDF5							
ITPR3	CRHR1	HBP1	PHC1	HMG20B	GDF6							
ITSN1	CRYM	HCFC1	PHC3	HPRT1	GDF7							
JAGN1	CYBSR4	HDAC1	PIAS1	HRAS	GDNF							
KCNS3	CYP11A1	HDAC3	PIBF1	HSP90AA1	GDPD5							
KDM5B	CYP17A1	HDAC8	PIF1	HSP90AB1	GFI1							
KIF5B	CYP19A1	HECA	PIK3C3	HSPAS5	GFR1							
KLF7	CYP26A1	HERC5	PIK3R4	HTRA2	GFR4							
LRP5	CYP26B1	HEXIM1	PINX1	ID1	GHRL							
LYN	CYP27A1	HEXIM2	PIWIL2	ID3	GJA1							
MCU	CYP27B1	HINFP	PIWIL3	ID4	GJC2							
MECP2	CYP27C1	HIPK2	PIWIL4	IDH2	GLDN							
MED1	CYP2D6	HIRA	PKD1	IER2	GLI2							
MIDN	CYP2S1	HMG20B	PKHD1	IFRD1	GLI3							
MYRIP	CYP3A4	HNRNPU	PKN2	IFT140	GNAT1							
NADK	CYP3A7	HRAS	PLAGL1	IFT20	GNAT2							
NFKB1	CYP46A1	HSF1	PLCB1	IFT27	GNRH1							
NLGN2	DDO	HSP90AA1	PLK3	IGSF9	GPM6B							
OXCT1	DHRS2	HSP90AB1	PLK4	IL6ST	GPR157							
PARK7	DIO1	HSPA1A	PLK5	ILK	GPR17							
PCSK6	DIO2	HSPA1B	PML	INPP5F	GPR173							
PCSK7	DIO3	HTRA2	PNPT1	IQGAP1	GPR183							
PFKFB2	DKK3	HTT	POLA1	IQSEC1	GPR371							
PFKL	DKKL1	HUS1	POLE2	IRS2	GPRC5B							
PHB	DOC2B	ID1	POM121	IRX2	GPRIN1							
PHPT1	DRD2	ID3	POM121C	ITGA3	GRIN1							
PIM3	DUOX1	ID4	POT1	ITGA6	GRIN2A							
PLEKHA1	DUOX2	IK	POU4F1	ITGB1	GRIP1							
POR	DUOXA1	ILK	PPM1D	ITM2C	GSX1							
PPARD	DUOXA2	INCENP	PPP1R1C	ITSN1	HAP1							
PPP3CB	ENPEP	ING1	PRDM11	JUN	HDAC10							
PPP5C	EPHAS	ING2	PRDM5	KANK1	HDAC9							
PRKCA	ESR1	ING4	PRDM9	KCTD11	HECW1							
PSMD9	EXOC3L1	INSR	PRIM1	KDM1A	HECW2							
PTPN11	FAM3D	INTS3	PRKAA2	KDM4C	HERC1							
RAB11B	FDXR	INTS7	PRKAG3	KIDINS220	HES2							
RAB11FIP1	FFAR2	IPOS	PRKR2B	KIF13B	HES7							
RAB11FIP3	FGA	IPO7	PRKCB	KIF1A	HEY1							
RAB11FIP5	FGB	IQGAP1	PRKCE	KIF3A	HHIP							
RAB1A	FGFR1	IRF6	PRR11	KIF5B	HMG20A							
RAC1	FKBP1B	ITGB1	PSMB10	KIF5C	HMG81							
RAF1	FOXA2	JMY	PSMB11	KLF7	HOOK3							
RAP1A	FOXD1	JTB	PSMB8	KRAS	HOXB3							
RDH11	FOXE1	JUN	PSMB9	KREMEN1	HOXC10							
RDH13	FOXL2	JUNB	PSMC1	LAMAS	HOXD1							
RDH14	FSHB	JUND	PSMC6	LAMB2	HOXD3							
RDH16	GAL	KANK2	PSME2	LDB1	HOXD9							
REST	GCG	KAT2A	PTEN	LDLR	HS6ST1							
RETSAT	GCNT4	KAT5	PTPRC	LEF1	IFT172							
SAFB	GDF9	KATNA1	RAB6C	LEMD2	IFT88							
SCARB1	GFI1	KCTD11	RAD51	LIG4	IGSF10							
SCPEP1	GHRHR	KHDRBS1	RAD51B	LIMK1	IHH							
SERP1	GHRL	KIAA0753	RAD51D	LIMK2	IL1RAPL1							
SGPL1	GIPR	KIF13A	RAD54L	LLGL1	IL33							
SIDT2	GJA1	KIF2A	RAD9B	LLPH	IL34							

Home Response				Cell Cycle				Neurogenesis				
UP	DOWN	NC HIGH RPKM	NC LOW RPKM	UP	DOWN	NC HIGH RPKM	NC LOW RPKM	UP	DOWN	NC HIGH RPKM	NC LOW RPKM	
29		398			127		1535		81		1314	
16	13	149	249	18	109	984	551	41	40	630	684	
SIN3A		GLP1R		KIF3A		RARA		LMTK2		INHBA		
SIRT3		GNB3		KIF3B		RASA1		LRP12		INPP5J		
SLC16A1		GPLD1		KLHDC3		RASSF4		LRP6		INSM1		
SLC25A5		GPR27		KLHL18		RBL1		LRP8		INSM2		
SLC2A1		GPR68		KLHL21		RBM7		LSM1		IRX3		
SLC4A4		GRP		KLHL22		REC8		LYN		IRX4		
SLCO4A1		HCAR2		KLHL9		RFP1		LYPLA2		IRX5		
SMAD2		HFE		KPNB1		RFWD3		MACF1		IRX6		
SMAD4		HNF1A		KRT18		RGS14		MAN2A1		ISL1		
SNAP23		HNF1B		L3MBTL2		RHEB		MANF		ISL2		
SNX19		HNF4A		LAMTOR1		RIF1		MAP1B		ITGA1		
SNX4		HSD17B1		LAMTOR2		RNASEH2B		MAP1S		ITGA4		
SOX4		HSD17B14		LAMTOR3		RNF112		MAP2K1		ITPKA		
SREBF1		HSD17B3		LATS1		RNF2		MAP3K13		ITSN2		
SRI		HSD17B6		LEMD2		ROPN1B		MAP4		JAK2		
STARD3		HSD17B7		LEMD3		RPA3		MAP4K4		JAM3		
STARD3NL		HSD17B8		LIG3		RPA4		MAPK1		KALRN		
STAT5B		HSD3B2		LIG4		RPRM		MAPK3		KATNB1		
STC2		HTR2C		LIN52		RPS27L		MAPK6		KCNIP2		
STUB1		IL11		LLGL1		RTTN		MAPK7		KCNJ10		
STX1A		ILDR2		LLGL2		RXFP3		MAPK8IP3		KEL		
STX4		INHA		LMLN		SASS6		MAPT		KIAA0319		
STXBP3		INHBA		LMNA		SDCCAG8		MARK2		KIF20B		
SYBU		INHBB		LMNB1		SETDB2		MBD1		KIF5A		
SYT7		IRS1		LPIN1		SF1		MBOAT7		KIRREL3		
TARDBP		ISL1		LPIN2		SH3GLB1		MDM2		KIT		
TM7SF3		ITPR1		LRP5		SHCBP1L		MECP2		KLF15		
TMF1		ITPR2		LRP6		SIPA1		MED1		KLK6		
TRERF1		IYD		LRRCC1		SIX3		MED12		KNDC1		
TRPM4		JAK2		LSM10		SLC26A8		MEGF8		L1CAM		
TSPO		KALRN		LYN		SLC38A9		METRN		LAMA1		
UBE2Q1		KCNB1		LZTS2		SLC39A5		METTL14		LAMA2		
VAMP8		KCNC2		MAD2L1BP		SLC6A4		METTL3		LAMA3		
YWHAH		KCNG2		MADD		SLFN11		MIB1		LAMC3		
ZMPSTE24		KCNJ11		MAEA		SLX4		MICALL1		LEP		
		KLK6		MAP2K1		SMARCD3		MICALL2		LEPR		
		LEP		MAP2K6		SMC1B		MINK1		LGALS1		
		LHB		MAP4		SMOC2		MMD		LGI4		
		LIF		MAP9		SMPD3		MOB2		LGR6		
		LMO3		MAPK1		SOX11		MOV10		LHFLP5		
		LRP1		MAPK13		SPAG8		MPP5		LHX2		
		LRP5L		MAPK14		SPAST		MTCH1		LHX3		
		LTBP4		MAPK3		SPC24		MTMR2		LHX4		
		MAFA		MAPK6		SPC25		MTOR		LHX5		
		MME		MAPK7		SPDYA		MTPN		LHX6		
		MTNR1B		MAPRE1		SPDYC		MUL1		LIF		
		MYB		MAPRE3		SPHK1		MXRA8		LINGO1		
		MYO5A		MARK4		SPICE1		MYCBP2		LMX1B		
		NDUFAF2		MASTL		SPIN2B		MYEF2		LPAR3		
		NKX6-1		MAU2		SPRY1		MYH10		LRIG2		
		NMB		MAX		SSTR5		MYO6		LRP1		
		NNM		MCM3		SSX2IP		NAB1		LRP2		
		NNAT		MCM4		STAG1		NAB2		LRP4		
		NOS2		MCM6		STAG3		NAGLU		LRRC4C		
		NPFF		MCM7		STAG3L1		NAP1L1		LRC7		
		NPPA						NAP1L2		LRTM2		
		NR0B2						NAPA		LRTOMT		

Home Response				Cell Cycle				Neurogenesis			
UP	DOWN	NC HIGH RPKM	NC LOW RPKM	UP	DOWN	NC HIGH RPKM	NC LOW RPKM	UP	DOWN	NC HIGH RPKM	NC LOW RPKM
29		398		127		1535		81		1314	
16	13	149	249	18	109	984	551	41	40	630	684
NR1D1		MCMBP	STAG3L2					LMTK2		INHBA	
NR5A1		MDC1	STAG3L3					LRP12		INPP5J	
OSM		MDM2	STARD9					LRP6		INSM1	
PASK		MECP2	STEAP3					LRP8		INSM2	
PAX8		MED1	STIL					LSM1		IRX3	
PCLO		MED25	STK10					LYN		IRX4	
PCSK1		MEN1	STK33					LYPLA2		IRX5	
PCSK4		MEPCE	STOX1					MACF1		IRX6	
PDGFRA		METTL3	STRADB					MAN2A1		ISL1	
PER1		MGA	STXBP4					MANF		ISL2	
PER2		MIF	SUGT1					MAP1B		ITGA1	
PLA2G6		MIS12	SUSD2					MAP1S		ITGA4	
PLB1		MITD1	SYCE2					MAP2K1		ITPKA	
PNPLA4		MLH1	SYCP3					MAP3K13		ITSN2	
POMC		MLST8	SYNE1					MAP4		JAK2	
PPARGC1A		MNAT1	TAF1					MAP4K4		JAM3	
PRKCE		MNT	TAF1L					MAPK1		KALRN	
PRLHR		MSH2	TAL1					MAPK3		KATNB1	
PTPRN		MSH6	TAS2R13					MAPK6		KCNIP2	
PTPRN2		MTA3	TBCE					MAPK7		KCNJ10	
RAB11FIP2		MTOR	TCFL2					MAPK8IP3		KEL	
RAB8B		MUC1	TDRD1					MAPT		KIAA0319	
RAPGEF3		MUS81	TDRD12					MARK2		KIF20B	
RAPGEF4		MX2	TDRD9					MBD1		KIF5A	
RASL10B		MYBBP1A	TDRKH					MBOAT7		KIRREL3	
RBP1		MYC	TERF1					MDM2		KIT	
RBP4		MYH10	TERF2					MECP2		KLF15	
RDH12		MYH9	TERT					MED1		KLK6	
RDH5		MYO19	TEX11					MED12		KNDC1	
REN		MZT1	TEX12					MEGF8		L1CAM	
RFX3		NAA10	TEX14					METRN		LAMA1	
RFX6		NAA50	TEX19					METTL14		LAMA2	
RIMS2		NACC2	TFDP2					METTL3		LAMA3	
RPE65		NASP	TFDP3					MIB1		LAMC3	
RPH3AL		NBN	TFGB1					MICALL1		LEP	
SCG5		NCAPD2	TGM1					MICALL2		LEPR	
SCT		NCOR1	THAP5					MINK1		LGALS1	
SIRT4		NDE1	THOC5					MMD		LGI4	
SLC16A10		NDEL1	TIPIN					MOB2		LGR6	
SLC16A2		NEDD9	TLK1					MOV10		LHFLP5	
SLC25A4		NEK4	TLK2					MPP5		LHX2	
SLC30A8		NEK6	TMEM67					MTCH1		LHX3	
SLC5A5		NEK7	TNF					MTMR2		LHX4	
SLC5A7		NF2	TNKS					MTOR		LHX5	
SLC9B2		NFE2L1	TP53					MTPN		LHX6	
SLCO1C1		NHP2	TP73					MUL1		LIF	
SMPD3		NIN	TRIM71					MXRA8		LINGO1	
SNAP25		NIPBL	TTBK1					MYCBP2		LMX1B	
SOX11		NLE1	TTC28					MYEF2		LPAR3	
SOX8		NME6	TTK					MYH10		LRIG2	
SRD5A1		NOLC1	TTN					MYO6		LRP1	
SRD5A2		NOP10	TTYH1					NAB1		LRP2	
SSTR5		NOTCH2	TUBA3C					NAB2		LRP4	
STAR		NPM1	TUBA3D					NAGLU		LRRC4C	
STXBP4		NR2F2	TUBA3E					NAP1L1		LRC7	
STXBP5L		NSFL1C	TUBA4B					NAP1L2		LRTM2	
SULT1B1		NSMCE2	TUBA8					NAPA		LRTOMT	

Steroid Receptor Signaling					Cell Cycle					Neurogenesis					
	UP	DOWN	NC HIGH RPKM	NC LOW RPKM		UP	DOWN	NC HIGH RPKM	NC LOW RPKM		UP	DOWN	NC HIGH RPKM	NC LOW RPKM	
	27	14	13	146		127	18	109	984		81	41	40	630	684
AR	ABCC2	ABCA2	AANAT			NSUN2	TUBAL3			NCDN	LTA				
ATP2B1	BRCA1	ABC A3	ABCC2			NUBP1	TUBB1			NCK1	LTK				
EGFR	HMG B2	ABHD2	ACR			NUDC	TUBB2A			NCK2	LZTS1				
ENG	KLF9	ADAM9	ACSBG1			NUDT15	TUBB2B			NCKAP1	MAG				
FOXO1	LBH	ADM	ACTA1			NUDT16	TUBB6			NCKIPSD	MAGI2				
HSD3B1	LOX	AIFM1	ADIPOQ			NUDT6	TUBE1			NCOA1	MAP1A				
IL1RN	NKX3-1	AKAP13	AGL			NUMA1	TUBG2			NCS1	MAP6				
PAK1	NR3C1	ALAD	AGXT			NUP133	TUBGCP3			NCSTN	MATN2				
PCK2	NR4A1	ARID1A	AKR1C3			NUP153	TUBGCP5			NDE1	MCF2				
PPARG	PER1	ARRB2	ALDH3A1			NUP160	TXNL4B			NDEL1	MDGA1				
PTGS2	PMEPA1	ATP1A1	ALPL			NUP188	UBD			NDRG1	MDGA2				
TGFB3	RARB	AXIN1	ANXA3			NUP205	UHRF1			NEDD4L	MEF2A				
THR8	TYMS	BAD	APOA2			NUP210	USP2			NF1	MEF2C				
UGT1A1	BCL2L11	AQP1				NUP214	USP3			NF2	MEIS1				
	BMP6	ARG1				NUP37	USP37			NFATC3	MET				
	CA2	ARNTL				NUP43	USP44			NFE2L1	MFSD2A				
	CAD	ASS1				NUP50	USP51			NFE2L2	MFSD8				
	CALCOCO1	ATP1A2				NUP54	VCP1P1			NFIB	MKS1				
	CALM3	ATP1A3				NUP62	VRK1			NGRN	MME				
	CALR	AVPR1A				NUP85	WDHD1			NIF3L1	MMP24				
	CARM1	BCHE				NUP88	WDR62			NIN	MNX1				
	CASP3	BCL2				NUP93	WDR76			NIPBL	MT3				
	CASP9	BGLAP				NUP98	WEE2			NME1	MTR				
	CBFB	BMP4				NUPR1	WHAMM			NME2	MYB				
	CBX3	BMP7				ODF2	WHAMMP3			NOTCH2	MYO16				
	CCND1	CALCR				OIPS	WNT10B			NOTCH3	MYO7A				
	CDKN1A	CATSPER2				OPTN	WNT4			NPTN	MYO9A				
	CFLAR	CATSPER3				ORC2	WNT9A			NR2F2	MYPN				
	CLDN4	CATSPER4				ORC3	WRAP53			NR2F6	NANOS1				
	CLOCK	CATSPERB				ORC5	WRN			NRBP2	NAV1				
	CNOT1	CATSPERG				OSGIN2	XRCC2			NRXN3	NAV2				
	CNOT2	CAV1				PAF1	YAF2			NSUN5	NAV3				
	CRY1	CCNE1				PAFAH1B1	YTHDC2			NUMB	NCAM1				
	CRY2	CD38				PAK4	ZBTB49			NUP133	NCKAP1L				
	CTNNB1	CDK7				PARD3	ZFHX3			OPA1	NDRG4				
	DAXX	CDO1				PAXIP1	ZFP36L2			OPHN1	NEDD4				
	DDIT4	CNGA3				PBRM1	ZNF655			P2RX4	NEFH				
	DDRGK1	COL1A1				PBX1	ZNF703			PAC SIN1	NEGR1				
	DDX17	CPS1				PCID2	ZWILCH			PAFAH1B1	NEK3				
	DDX5	CSN1S1				PCM1				PAK2	NEO1				
	DDX54	CYBA				PCNA				PAK4	NEUROD4				
	DNAJA1	CYBB				PCNP				PAK6	NEVN				
	DSG2	CYP7B1				PCNT				PALLD	NFASC				
	DUSP1	DAB2				PDCD2L				PAQR3	NFAT5				
	EDN1	DNMT3B				PDCD4				PARD3	NFATC1				
	EGLN2	DSG1				PDCD6IP				PBX1	NFATC2				
	EIF4E	ENG				PDSSA				PBX2	NFATC4				
	EIF4EBP1	EPO				PDSSB				PBX3	NGEF				
	EP300	ESR1				PDXP				PCM1	NGFR				
	ERRFI1	ESR2				PEA15				PDLIM7	NKD1				
	ESRRA	ESRRB				PELO				PEX13	NKX2-1				
	FBXO32	ESRRG				PES1				PEX7	NKX2-2				
	FKBP4	FAM107A				PGGT1B				PHGDH	NKX2-5				
	FOXA1	FHL2				PHACTR4				PICALM	NKX2-8				
	FOXP1	FLT3				PHB2				PICK1	NKX6-1				
	GBA	FOSB				PHF13				PIGT	NKX6-2				
	GLB1	FOSL1				PHF20				PIK3CB	NLGN1				

Steroid Receptor Signaling						Cell Cycle						Neurogenesis					
UP		DOWN		NC RPKM		UP		DOWN		NC RPKM		UP		DOWN		NC RPKM	
27		301				127		1535				81		1314			
14	13	146	155			18	109	984	551			41	40	630	684		
GOT1		FOXH1				PHF23						PIK3R1		NLGN3			
GSTP1		FOXO1				PHF8						PIN1		NLGN4X			
HDAC1		GHRHR				PHGDH						PITPNNA		NNAT			
HDAC6		GIB2				PHIP						PLAA		NOS1			
HNRNPU		GNRH1				PIAS4						PLCG1		NOTCH1			
IDH1		GPAM				PIM2						PLK2		NPHP4			
IGFBP2		GPR83				PIM3						PLXNA1		NPTX1			
KANK2		GRIP1				PIN1						PLXNA3		NR1D1			
KATS		HNF4A				PKD2						PLXNB1		NR2E1			
KCTD6		HNF4G				PKIA						PLXNB2		NR2E3			
KDM3A		HNMT				PKP4						PPP1CC		NR2F1			
KDM5D		HSD3B2				PLD6						PPP1R9B		NR4A2			
KRAS		HTR1B				PLK2						PPP2RB		NR4A3			
LATS1		ICAM1				PLRG1						PPP3CB		NRAS			
LEF1		IGFBP7				PMF1						PPP3R1		NRCAM			
MDM2		ISL1				POC5						PPT1		NRK			
MED1		JAK2				POGZ						PQBP1		NRL			
NCOA1		LMO3				POLA2						PRKCA		NN1L			
NCOA2		LOX				POLD2						PRKCH		NRP2			
NCOA3		METTL21C				POLD3						PRKCI		NRTN			
NCOA4		MSTN				POLD4						PRKCZ		NRXN1			
NCOR1		MYOD1				POLDIP2						PRKD1		NTF3			
NCOR2		NEDD4				POLE						PRMT1		NTF4			
NPC1		NKX2-2				POLE3						PRMT5		NTN1			
NR1D2		NODAL				POLE4						PRPF19		NTN3			
NR1H2		NOTCH1				PPAT						PSAP		NTN5			
NR2C1		NPAS4				PPM1A						PSEN1		NTNG2			
NR2C2		NR0B2				PPM1G						PTCH1		NTRK2			
NR2F2		NR1D1				PPME1						PTK2		NTRK3			
NR2F6		NR1H3				PPP1CA						PTK2B		NUMBL			
NR3C2		NR1I2				PPP1CB						PTK7		OLFM1			
NRIP1		NR1I3				PPP1CC						PTPN11		OLIG1			
PARK7		NR2E1				PPP1R10						PTPN9		OLIG3			
PARP1		NR2E3				PPP1R12A						PTPRA		OMG			
PCNA		NR2F1				PPP1R12B						PTPRF		OMP			
PGRMC2		NR4A2				PPP1R13B						PTPRK		ONECUT2			
PHB		NR4A3				PPP1R15A						PTPRM		OPALIN			
PHB2		NR5A1				PPP1R9B						PTPRS		OPRM1			
PIAS2		NR5A2				PPP2CA						RAB10		OSTN			
PPARD		NR6A1				PPP2CB						RAB11A		OTP			
PPP1R9B		NTRK3				PPP2R1A						RAB13		P2RY12			
PPP5C		OR51E2				PPP2R1B						RAB17		PARD6B			
PRMT2		OXT				PPP2R2A						RAB21		PAX2			
RAN		OXTR				PPP2R2D						RAB35		PAX6			
RARG		PADI2				PPP2R5A						RAB3A		PBX4			
RB1		PAPPA				PPP2R5B						RAB8A		PCDH12			
RBBP7		PAQR7				PPP2R5C						RAC1		PCP4			
RBFOX2		PAQR8				PPP2R5D						RAC3		PCSK9			
RELA		PCK1				PPP2R5E						RACGAP1		PDE6C			
REST		PDCD7				PPP5C						RANBP9		PDZD7			
RHOA		PER1				PPP6C						RAP1A		PER2			
RNF14		PFKFB1				PRCC						RAPGEF1		PHACTR1			
RNF4		PGR				PRIM2						RAPGEF2		PHOX2A			
RNF6		PIAS1				PRKAA1						RB1		PIK3CA			
RPS6KB1		POU4F2				PRKAB1						RBFOX2		PIK3CD			
RWDD1		PPARA				PRKAB2						RBPJ		PITX2			
RXRA		PPARGC1A				PRKACA						RDH13		PLA2G10			

Steroid Receptor Signaling					
UP	DOWN	NC		NC	
		HIGH RPKM	LOW RPKM	HIGH RPKM	LOW RPKM
27		301			
14	13	146	155		
	RXRB	PPARGC1B			
	SAFB	PTAFR			
	SAFB2	PTGER2			
	SDC1	PTN			
	SIRT1	PTPRU			
	SKP2	RAMP2			
	SMARCA4	RARA			
	SMYD3	RARB			
	SRC	RORA			
	SREBF1	RORB			
	STRN3	RORC			
	TADA3	RUNX1			
	TAF7	SCGB2A1			
	TFAP4	SCGB2A2			
	TGFBR2	SERPINF1			
	THRA	SLT2			
	TSPO	SLT3			
	TXNIP	SOX10			
	UBA5	SOX30			
	UBE2I	SPARC			
	UBE2L3	SRDSA1			
	UBE3A	SSTR2			
	UBR5	SSTR5			
	UFM1	STAR			
	USP8	TFPI			
	WBP2	TGFB1			
	WNT7B	TGFB1I1			
	YAP1	TGFB3			
	YWHAH	TH			
	ZBTB7A	TLR2			
	ZFP36	TNF			
	ZFP36L1	TP63			
		TPH2			
		TRIM63			
		TRIM68			
		TRIP4			
		UCN			
		UCP3			
		UFSP2			
		VDR			
		ZFP36L2			

Cell Cycle					
UP	DOWN	NC		NC	
		HIGH RPKM	LOW RPKM	HIGH RPKM	LOW RPKM
127		1535			
18	109	984	551		
		PRKACB			
		PRKAG1			
		PRKAR1A			
		PRKCA			
		PRKCD			
		PRKDC			
		PRMT1			
		PRMT2			
		PRMT5			
		PRNP			
		PRPF19			
		PRPF40A			
		PRRS			
		PSMA1			
		PSMA2			
		PSMA3			
		PSMA4			
		PSMA5			
		PSMA6			
		PSMA7			
		PSMB1			
		PSMB2			
		PSMB3			
		PSMB4			
		PSMB5			
		PSMB6			
		PSMB7			
		PSMC2			
		PSMC3			
		PSMC4			
		PSMC5			
		PSMD1			
		PSMD10			
		PSMD11			
		PSMD12			
		PSMD13			
		PSMD14			
		PSMD2			
		PSMD3			
		PSMD4			
		PSMD5			
		PSMD6			
		PSMD7			
		PSMD8			
		PSMD9			
		PSME1			
		PSME3			
		PSME4			
		PSMF1			
		PSMG2			
		PTCH1			
		PTP4A1			
		PTPN11			
		PTPN3			
		PTPN6			
		PTPRK			
		PTTG2			

Neurogenesis					
UP	DOWN	NC		NC	
		HIGH RPKM	LOW RPKM	HIGH RPKM	LOW RPKM
81		1314			
41	40	630	684		
		RELA	PLA2G3		
		RERE	PLA41		
		REST	PLK5		
		RGS3	PLXNA2		
		RHOA	PLXNA4		
		RHOD	PLXNB3		
		RHOG	PLXNC1		
		RHOH	PLXND1		
		RNF10	PMP22		
		RNF6	POU3F1		
		ROCK1	POU3F2		
		ROGDI	POU4F1		
		RRN3	POU4F2		
		RTN4	POU4F3		
		RYK	PPP1R9A		
		SCARB2	PPP3CC		
		SCRIB	PPP3R2		
		SCYL1	PRDM1		
		SDC2	PRDM12		
		SDC4	PRDM13		
		SEC24B	PRDM16		
		SECISBP2	PRDM6		
		SEMA3B	PRDM8		
		SEMA3F	PREX1		
		SEMA4A	PREX2		
		SEMA4B	PRKG1		
		SEMA4C	PRRX1		
		SEMA4D	PRX		
		SEMA6A	PSD		
		SERpine2	PSPN		
		SETX	PTEN		
		SGK1	PTN		
		SH3KBP1	PTPRD		
		SH3RF1	PTPRG		
		SHC1	PTPRO		
		SIAH1	PTPRZ1		
		SIN3A	RAC2		
		SIPA1L1	RAP1GAP2		
		SIRT2	RAPH1		
		SIX1	RARA		
		SKI	RARB		
		SKIL	RASA1		
		SLC11A2	RASAL1		
		SLC25A46	RASGRF1		
		SLC44A4	RASSF10		
		SLC44A7	RELN		
		SLC9A3R1	RET		
		SLIT1	RGMA		
		SMAD4	RGS14		
		SMARCE1	RHEB		
		SMO	RIMS1		
		SMURF1	RIMS2		
		SNAPIN	RND1		
		SNPH	RND2		
		SNW1	RNF112		
		SNX3	RNF157		
		SOD1	RNF165		

Cell Cycle			
UP	DOWN	NC HIGH RPKM	NC LOW RPKM
<b>127</b>		<b>1535</b>	
18	109	984	551
PUM1			
RAB11A			
RAB11FIP3			
RAB11FIP4			
RAB1A			
RAB1B			
RAB2A			
RAB35			
RAB8A			
RABGAP1			
RACGAP1			
RAD1			
RAD17			
RAD21			
RAD23A			
RAD50			
RAD54B			
RAD9A			
RAE1			
RALA			
RALB			
RAN			
RANBP1			
RANBP2			
RANGAP1			
RASSF1			
RASSF2			
RB1			
RB1CC1			
RBPP4			
RBPP7			
RBPP8			
RBL2			
RBM14			
RBM38			
RBX1			
RCBTB1			
RCC1			
RCC2			
RDX			
RECQL5			
REEP3			
REEP4			
RFC1			
RFC2			
RFC4			
RFC5			
RHOA			
RHOB			
RHOC			
RHOU			
RING1			
RINT1			
RIOK2			
RIPK1			
RMI1			
RNF167			

Neurogenesis			
UP	DOWN	NC HIGH RPKM	NC LOW RPKM
<b>81</b>		<b>1314</b>	
41	40	630	684
SORL1		ROBO2	
SOX4		ROBO3	
SPAG9		ROBO4	
SPEN		ROCK2	
SPG11		ROM1	
SPINT1		ROR1	
SPOCK1		ROR2	
SPTAN1		RORA	
SPTBN1		RORB	
SPTBN2		RP1L1	
SRC		RPE65	
SRF		RPGRIPI	
SRGAP2		RPGRIPI1	
SRRT		RPS6KA5	
SS18L1		RSP02	
SS18L2		RTN4IP1	
STAT3		RTN4R	
STK11		RTN4RL1	
STK24		RTN4RL2	
STK25		RUFY3	
STRN		RUNX1	
STX3		RUNX2	
STXBP1		S1PR5	
STYXL1		SAMD14	
SUFU		SARM1	
SUN1		SATB2	
SUN2		SCARF1	
SUZ12		SCLT1	
SYNE2		SCN1B	
SYT17		SCRT1	
SZT2		SCYL3	
TANC2		SDCCAG8	
TAOK1		SDK1	
TAOK2		SDK2	
TBC1D24		SEMA3A	
TBCD		SEMA3C	
TCF12		SEMA3D	
TCF3		SEMA3E	
TCTN1		SEMA3G	
TDP2		SEMA4F	
TEAD3		SEMA4G	
THOC2		SEMA5B	
TIMP2		SEMA6B	
TMEM106B		SEMA6C	
TMEM30A		SEMA6D	
TMEM98		SEMA7A	
TNFRSF12A		SERPINF1	
TOP2B		SEZ6	
TOPORS		SFRP2	
TOR1A		SH3GL2	
TPPP		SH3GL3	
TPRN		SH3TC2	
TRAK1		SHANK2	
TRAK2		SHANK3	
TRAPP4		SHC3	
TRAPP9		SHOX2	
TRIM11		SIX3	

Cell Cycle			
UP	DOWN	NC HIGH RPKM	NC LOW RPKM
		127	1535
18	109	984	551
	RNF168		
	RNF4		
	RNF8		
	ROCK1		
	RPA2		
	RPL23		
	RPL24		
	RPL26		
	RPRD1B		
	RPS15A		
	RPS27A		
	RPS3		
	RPS6		
	RPS6KA1		
	RPS6KA2		
	RPS6KA3		
	RPS6KB1		
	RPTOR		
	RRAGA		
	RRAGB		
	RRAGC		
	RRAGD		
	RRM1		
	RRP8		
	RRS1		
	RSF1		
	RSPH1		
	RTKN		
	RUVBL1		
	RUVBL2		
	RYBP		
	SAC3D1		
	SBDS		
	SCRIB		
	SDCBP		
	SEC13		
	SEH1L		
	SENP2		
	SENP5		
	SENP6		
	SERTAD1		
	SET		
	SETD2		
	SETMAR		
	SFN		
	SFPQ		
	SGSM3		
	SH2B1		
	SIAH1		
	SIAH2		
	SIK1		
	SIN3A		
	SIRT1		
	SIRT2		
	SIRT7		
	SKIL		
	SKP1		

Neurogenesis			
UP	DOWN	NC HIGH RPKM	NC LOW RPKM
		81	1314
41	40	630	684
	TRIM32	SIX4	
	TRIO	SLC12A5	
	TRIOBP	SLC1A3	
	TRIP11	SLC4A10	
	TSC1	SLC6A4	
	TSKU	SLC8A3	
	TSPO	SLC9A6	
	TTL	SLIT1	
	TUBB3	SLIT2	
	TUG1	SLIT3	
	TULP3	SLITRK3	
	TWF1	SLITRK4	
	TWF2	SLITRK5	
	UBA6	SLITRK6	
	UBB	SMARCD3	
	UBE3A	SNAP25	
	UBE4B	SOS1	
	UHMK1	SOX10	
	ULK1	SOX11	
	UNK	SOX6	
	UQCRCQ	SOX8	
	USP21	SPAST	
	USP33	SPINK5	
	USP9X	SPTB	
	UST	SPTBN4	
	VANGL2	SPTBN5	
	VAPA	SRCIN1	
	VASP	SRGAP1	
	VAX2	STAP1	
	VCL	STAR	
	VEGFA	STMN2	
	WASF3	STMN3	
	WASL	STMN4	
	WDR1	STX1B	
	WDR5	SYN1	
	WEE1	SYNGAP1	
	WNK1	SYT2	
	WNT11	SYT4	
	WNT5A	TAL1	
	WNT5B	TBC1D23	
	WNT7B	TBR1	
	XBP1	TBX20	
	XRCC5	TBX6	
	XRN2	TCF4	
	YAP1	TERT	
	YTHDF1	TGFB1	
	YTHDF2	TH	
	YWHAE	TIAM1	
	YWHAH	TIAM2	
	YWHAH	TLR2	
	YWHAZ	TLR4	
	ZC4H2	TLX2	
	ZFYVE27	TMC1	
	ZHX2	TMEFF1	
	ZMIZ1	TMEM108	
	ZMYND8	TMEM132E	
	ZNF335	TNF	

Cell Cycle			
UP	DOWN	NC HIGH RPKM	NC LOW RPKM
<b>127</b>		<b>1535</b>	
18	109	984	551
SKP2			
SLC16A1			
SLC2A8			
SLC9A3R1			
SMAD3			
SMARCA5			
SMARCA1			
SMARCB1			
SMC1A			
SMC3			
SMC4			
SMC5			
SND1			
SNX18			
SNX33			
SNX9			
SON			
SOX15			
SOX4			
SPEC1L			
SPIN1			
SPIRE1			
SPIRE2			
SPTBN1			
SRC			
SRPK2			
SRSF5			
SSNA1			
STAG2			
STAG3L4			
STAMBPP			
STAT3			
STAT5B			
STK11			
STRADA			
SUMO1			
SUN1			
SUN2			
SUV39H1			
SUV39H2			
SUZ12			
SVIL			
SYCP2			
SYF2			
SYNE2			
TACC1			
TACC2			
TADA3			
TAF10			
TAF2			
TAF6			
TAOK1			
TAOK2			
TARDBP			
TBCD			
TBRG1			
TBRG4			

Neurogenesis			
UP	DOWN	NC HIGH RPKM	NC LOW RPKM
<b>81</b>		<b>1314</b>	
41	40	630	684
ZNF609			TNFRSF1B
ZSWIM4			TNIK
ZSWIM6			TOX
			TP53
			TP73
			TREM2
			TRIM46
			TRIM67
			TRPC5
			TRPM1
			TRPV4
			TTBK1
			TTC21B
			TTL1
			TUBB2A
			TUBB2B
			TULP1
			TWIST1
			UCHL1
			UCN
			ULK4
			UNC13A
			UNC5A
			UNC5C
			USH1G
			USH2A
			VASH2
			VAX1
			VEGFC
			VIM
			VTN
			WASF1
			WDPCP
			WDR36
			WDR62
			WNT1
			WNT10B
			WNT16
			WNT2B
			WNT3
			WNT3A
			WNT4
			WNT8B
			WNT9A
			WNT9B
			XK
			XRCC2
			ZDHHC15
			ZEB1
			ZEB2
			ZFHX2
			ZFHX3
			ZNF488
			ZNF536
			ZNF804A
			ZSWIMS

Cell Cycle			
UP	DOWN	NC HIGH RPKM	NC LOW RPKM
127		1535	
18	109	984	551
TEN1			
TERF2IP			
TET2			
TFAP4			
TFDP1			
THAP1			
THOC1			
TIMELESS			
TIMP2			
TINF2			
TIPRL			
TK1			
TMEM14B			
TMEM8B			
TMOD3			
TMPO			
TNFAIP3			
TNKS1BP1			
TNPO1			
TOM1L1			
TOM1L2			
TOP2B			
TOP3A			
TOPBP1			
TP53BP1			
TP53BP2			
TP53I13			
TP53INP1			
TPD52L1			
TPR			
TPRA1			
TREX1			
TRIAP1			
TRIM32			
TRIM35			
TRIM37			
TRIOBP			
TRNP1			
TSC1			
TSC2			
TSG101			
TSPYL2			
TTC19			
TTL			
TTLL12			
TUBA1B			
TUBA1C			
TUBA4A			
TUBB			
TUBB3			
TUBD1			
TUBG1			
TUBGCP2			
TUBGCP4			
TUBGCP6			
TUSC2			
TXLNG			

Cell Cycle			
UP	DOWN	NC HIGH RPKM	NC LOW RPKM
127		1535	
18	109	984	551
TXNIP			
TXNL4A			
UBA3			
UBA52			
UBB			
UBC			
UBE2B			
UBE2E1			
UBE2E2			
UBE2I			
UBE2L3			
UBE2N			
UBE2V2			
UBR2			
UBXN2B			
UHMK1			
UHRF2			
UIMC1			
UNC119			
UPF1			
URGCP			
USO1			
USP16			
USP19			
USP22			
USP28			
USP33			
USP39			
USP47			
USP8			
USP9X			
UTP14C			
UVRAG			
UXT			
VASH1			
VCP			
VPS4A			
VPS4B			
VRK2			
WAC			
WASL			
WDR6			
WEE1			
WIZ			
WNT5A			
WRAP73			
WTAP			
XPC			
XPO1			
YEATS4			
YTHDF2			
YWHAB			
YWHAE			
YWHAG			
YWHAH			
YWHAQ			
YWHAZ			

Cell Cycle					
UP	DOWN	NC		NC	
		HIGH RPKM	LOW RPKM		
127		1535			
18	109	984	551		
YY1AP1 ZBTB17 ZC3HC1 ZFP36L1 ZFVE19 ZFVE26 ZMPSTE24 ZMYND11 ZNF16 ZNF207 ZNF268 ZNF318 ZNF385A ZNF503 ZNF830 ZW10					

**Table S2.** Selected pathway categories of interest with numbers of differentially expressed genes in APDT-signature from PDX PCSD1 organoids.

Category	Fold Enrichment	P-value	Differential (# Genes)			%	NO CHANGE (% Genes)			Total # Genes with Reads	
			UP	DOWN	Total		HIGH	LOW	Total		
Interferon Signaling	4.9	2.0E-08	0	18	18	22.8	40	21	61	77.2	79
Cell Cycle	1.7	1.5E-07	18	109	127	7.8	985	519	1,504	92.2	1,631
Circadian Clock	1.6	9.3E-02	7	8	15	7.2	113	79	192	92.8	207
Prostate Stem /Progenitor	2.6	1.1E-02	5	3	8	12.1	22	36	58	87.9	66
NEPC /Neurogenic	2.2	1.9E-03	6	14	20	10.0	85	95	180	90.0	200
Neurogenesis	1.3	3.3E-03	41	40	81	5.9	627	655	1,282	94.1	1,363
Axon Guidance	2.4	3.2E-02	12	1	13	11.1	50	54	104	89.9	117
Hormone Response	1.5	3.3E-02	16	13	29	7.0	149	236	385	93.0	414
Steroid Receptor Signaling	1.8	3.2E-02	14	13	27	8.4	146	148	294	91.6	321
ALL	1.0	na	269	518	787	4.6	7,581	8,63	1,621	95.4	17,004

## References

1. Siegel, R. L.; Miller, K. D.; Fuchs, H. E.; Jemal, A., Cancer Statistics, 2021. *CA Cancer J Clin* **2021**, *71*, (1), 7-33.
2. Ahlering, T.; Huynh, L. M.; Kaler, K. S.; Williams, S.; Osann, K.; Joseph, J.; Lee, D.; Davis, J. W.; Abaza, R.; Kaouk, J.; Patel, V.; Kim, I. Y.; Porter, J.; Hu, J. C., Unintended consequences of decreased PSA-based prostate cancer screening. *World J Urol* **2019**, *37*, (3), 489-496.
3. Teo, M. Y.; Rathkopf, D. E.; Kantoff, P., Treatment of Advanced Prostate Cancer. *Annu Rev Med* **2019**, *70*, 479-499.
4. Kim, T. J.; Lee, Y. H.; Koo, K. C., Current Status and Future Perspectives of Androgen Receptor Inhibition Therapy for Prostate Cancer: A Comprehensive Review. *Biomolecules* **2021**, *11*, (4).
5. Labriola, M. K.; Atiq, S.; Hirshman, N.; Bitting, R. L., Management of men with metastatic castration-resistant prostate cancer following potent androgen receptor inhibition: a review of novel investigational therapies. *Prostate Cancer Prostatic Dis* **2021**, *24*, (2), 301-309.
6. Lin, H.; Liu, Q.; Zeng, X.; Yu, W.; Xu, G., Pembrolizumab with or without enzalutamide in selected populations of men with previously untreated metastatic castration-resistant prostate cancer harbouring programmed cell death ligand-1 staining: a retrospective study. *BMC Cancer* **2021**, *21*, (1), 399.

7. Sperger, J. M.; Emamekhoo, H.; McKay, R. R.; Stahlfeld, C. N.; Singh, A.; Chen, X. E.; Kwak, L.; Gilsdorf, C. S.; Wolfe, S. K.; Wei, X. X.; Silver, R.; Zhang, Z.; Morris, M. J.; Bubley, G.; Feng, F. Y.; Scher, H. I.; Rathkopf, D.; Dehm, S. M.; Choueiri, T. K.; Halabi, S.; Armstrong, A. J.; Wyatt, A. W.; Taplin, M. E.; Zhao, S. G.; Lang, J. M., Prospective Evaluation of Clinical Outcomes Using a Multiplex Liquid Biopsy Targeting Diverse Resistance Mechanisms in Metastatic Prostate Cancer. *J Clin Oncol* **2021**, JCO2100169.
8. Jillson, L. K.; Rider, L. C.; Rodrigues, L. U.; Romero, L.; Karimpour-Fard, A.; Nieto, C.; Gillette, C.; Torkko, K.; Danis, E.; Smith, E. E.; Nolley, R.; Peehl, D. M.; Lucia, M. S.; Costello, J. C.; Cramer, S. D., Loss Drives Enhanced Androgen Signaling and Independently Confers Risk of Recurrence in Prostate Cancer with Joint Loss of. *Mol Cancer Res* **2021**, 19, (7), 1123-1136.
9. Oster, G.; Lamerato, L.; Glass, A. G.; Richert-Boe, K. E.; Lopez, A.; Chung, K.; Richhariya, A.; Dodge, T.; Wolff, G. G.; Balakumaran, A.; Edelsberg, J., Natural history of skeletal-related events in patients with breast, lung, or prostate cancer and metastases to bone: a 15-year study in two large US health systems. *Support Care Cancer* **2013**, 21, (12), 3279-86.
10. Logothetis, C.; Morris, M. J.; Den, R.; Coleman, R. E., Current perspectives on bone metastases in castrate-resistant prostate cancer. *Cancer Metastasis Rev* **2018**, 37, (1), 189-196.
11. Garnero, P.; Buchs, N.; Zekri, J.; Rizzoli, R.; Coleman, R. E.; Delmas, P. D., Markers of bone turnover for the management of patients with bone metastases from prostate cancer. *Br J Cancer* **2000**, 82, (4), 858-64.
12. Berchuck, J. E.; Viscuse, P. V.; Beltran, H.; Aparicio, A., Clinical considerations for the management of androgen indifferent prostate cancer. *Prostate Cancer Prostatic Dis* **2021**.
13. Crona, D. J.; Whang, Y. E., Androgen Receptor-Dependent and -Independent Mechanisms Involved in Prostate Cancer Therapy Resistance. *Cancers (Basel)* **2017**, 9, (6).
14. Coleman, R. E.; Croucher, P. I.; Padhani, A. R.; Clézardin, P.; Chow, E.; Fallon, M.; Guise, T.; Colangeli, S.; Capanna, R.; Costa, L., Bone metastases. *Nat Rev Dis Primers* **2020**, 6, (1), 83.
15. Hussain, A.; Tripathi, A.; Pieczonka, C.; Cope, D.; McNatty, A.; Logothetis, C.; Guise, T., Bone health effects of androgen-deprivation therapy and androgen receptor inhibitors in patients with nonmetastatic castration-resistant prostate cancer. *Prostate Cancer Prostatic Dis* **2020**.
16. Brady, L.; Kriner, M.; Coleman, I.; Morrissey, C.; Roudier, M.; True, L. D.; Gulati, R.; Plymate, S. R.; Zhou, Z.; Birditt, B.; Meredith, R.; Geiss, G.; Hoang, M.; Beechem, J.; Nelson, P. S., Inter- and intra-tumor heterogeneity of metastatic prostate cancer determined by digital spatial gene expression profiling. *Nat Commun* **2021**, 12, (1), 1426.
17. Sobel, R. E.; Sadar, M. D., Cell lines used in prostate cancer research: a compendium of old and new lines--part 1. *J Urol* **2005**, 173, (2), 342-59.
18. Namekawa, T.; Ikeda, K.; Horie-Inoue, K.; Inoue, S., Application of Prostate Cancer Models for Preclinical Study: Advantages and Limitations of Cell Lines, Patient-Derived Xenografts, and Three-Dimensional Culture of Patient-Derived Cells. *Cells* **2019**, 8, (1).
19. Raheem, O.; Kulidjian, A. A.; Wu, C.; Jeong, Y. B.; Yamaguchi, T.; Smith, K. M.; Goff, D.; Leu, H.; Morris, S. R.; Cacalano, N. A.; Masuda, K.; Jamieson, C. H.; Kane, C. J.; Jamieson, C. A., A novel patient-derived intra-femoral xenograft model of bone metastatic prostate cancer that recapitulates mixed osteolytic and osteoblastic lesions. *J Transl Med* **2011**, 9, 185.
20. Godebu, E.; Muldong, M.; Strasner, A.; Wu, C. N.; Park, S. C.; Woo, J. R.; Ma, W.; Liss, M. A.; Hirata, T.; Raheem, O.; Cacalano, N. A.; Kulidjian, A. A.; Jamieson, C. A., PCSD1, a new patient-derived model of bone metastatic prostate cancer, is castrate-resistant in the bone-niche. *J Transl Med* **2014**, 12, 275.
21. Nguyen, H. M.; Vessella, R. L.; Morrissey, C.; Brown, L. G.; Coleman, I. M.; Higano, C. S.; Mostaghel, E. A.; Zhang, X.; True, L. D.; Lam, H. M.; Roudier, M.; Lange, P. H.; Nelson, P. S.; Corey, E., LuCaP Prostate Cancer Patient-Derived Xenografts Reflect the Molecular Heterogeneity of Advanced Disease and Serve as Models for Evaluating Cancer Therapeutics. *Prostate* **2017**, 77, (6), 654-671.
22. Navone, N. M.; van Weerden, W. M.; Vessella, R. L.; Williams, E. D.; Wang, Y.; Isaacs, J. T.; Nguyen, H. M.; Culig, Z.; van der Pluijm, G.; Rentsch, C. A.; Marques, R. B.; de Ridder, C. M. A.; Bubendorf, L.; Thalmann, G. N.; Brennen, W. N.; Santer, F. R.; Moser, P. L.; Shepherd, P.; Efstatithiou, E.; Xue, H.; Lin, D.; Buijs, J.; Bosse, T.; Collins, A.; Maitland, N.; Buzzà, M.; Koussou, M.; Achttman, A.; Taylor, R. A.; Risbridger, G.; Corey, E., Movember GAP1 PDX project: An international collection of serially transplantable prostate cancer patient-derived xenograft (PDX) models. *Prostate* **2018**, 78, (16), 1262-1282.
23. Klein, K. A.; Reiter, R. E.; Redula, J.; Moradi, H.; Zhu, X. L.; Brothman, A. R.; Lamb, D. J.; Marcelli, M.; Belldegrun, A.; Witte, O. N.; Sawyers, C. L., Progression of metastatic human prostate cancer to androgen independence in immunodeficient SCID mice. *Nat Med* **1997**, 3, (4), 402-8.
24. Corey, E.; Quinn, J. E.; Vessella, R. L., A novel method of generating prostate cancer metastases from orthotopic implants. *Prostate* **2003**, 56, (2), 110-4.
25. Karthaus, W. R.; Iaquinta, P. J.; Drost, J.; Gracanin, A.; van Boxtel, R.; Wongvipat, J.; Dowling, C. M.; Gao, D.; Begthel, H.; Sachs, N.; Vries, R. G. J.; Cuppen, E.; Chen, Y.; Sawyers, C. L.; Clevers, H. C., Identification of multipotent luminal progenitor cells in human prostate organoid cultures. *Cell* **2014**, 159, (1), 163-175.
26. Drost, J.; Karthaus, W. R.; Gao, D.; Driehuis, E.; Sawyers, C. L.; Chen, Y.; Clevers, H., Organoid culture systems for prostate epithelial and cancer tissue. *Nat Protoc* **2016**, 11, (2), 347-58.
27. van de Wetering, M.; Frances, H. E.; Francis, J. M.; Bounova, G.; Iorio, F.; Pronk, A.; van Houdt, W.; van Gorp, J.; Taylor-Weiner, A.; Kester, L.; McLaren-Douglas, A.; Blokker, J.; Jaksani, S.; Bartfeld, S.; Volckman, R.; van Sluis, P.; Li, V. S.; Seepo, S.; Sekhar Pedamallu, C.; Cibulskis, K.; Carter, S. L.; McKenna, A.; Lawrence, M. S.; Lichtenstein, L.; Stewart, C.; Koster, J.; Versteeg, R.; van Oudenaarden, A.; Saez-Rodriguez, J.; Vries, R. G.; Getz, G.; Wessels, L.; Stratton, M. R.; McDermott, U.; Meyerson, M.;

- Garnett, M. J.; Clevers, H., Prospective derivation of a living organoid biobank of colorectal cancer patients. *Cell* **2015**, *161*, (4), 933-45.
28. Chua, C. W.; Shibata, M.; Lei, M.; Toivanen, R.; Barlow, L. J.; Bergren, S. K.; Badani, K. K.; McKiernan, J. M.; Benson, M. C.; Hibshoosh, H.; Shen, M. M., Single luminal epithelial progenitors can generate prostate organoids in culture. *Nat Cell Biol* **2014**, *16*, (10), 951-61, 1-4.
  29. Agarwal, S.; Hynes, P. G.; Tillman, H. S.; Lake, R.; Abou-Kheir, W. G.; Fang, L.; Casey, O. M.; Ameri, A. H.; Martin, P. L.; Yin, J. J.; Iaquinta, P. J.; Karthaus, W. R.; Clevers, H. C.; Sawyers, C. L.; Kelly, K., Identification of Different Classes of Luminal Progenitor Cells within Prostate Tumors. *Cell Rep* **2015**, *13*, (10), 2147-58.
  30. Gao, D.; Vela, I.; Sboner, A.; Iaquinta, P. J.; Karthaus, W. R.; Gopalan, A.; Dowling, C.; Warjala, J. N.; Undvall, E. A.; Arora, V. K.; Wongvipat, J.; Kossai, M.; Ramazanoglu, S.; Barboza, L. P.; Di, W.; Cao, Z.; Zhang, Q. F.; Sirota, I.; Ran, L.; MacDonald, T. Y.; Beltran, H.; Mosquera, J. M.; Touijer, K. A.; Scardino, P. T.; Laudone, V. P.; Curtis, K. R.; Rathkopf, D. E.; Morris, M. J.; Danila, D. C.; Slovin, S. F.; Solomon, S. B.; Eastham, J. A.; Chi, P.; Carver, B.; Rubin, M. A.; Scher, H. I.; Clevers, H.; Sawyers, C. L.; Chen, Y., Organoid cultures derived from patients with advanced prostate cancer. *Cell* **2014**, *159*, (1), 176-187.
  31. Puca, L.; Bareja, R.; Prandi, D.; Shaw, R.; Benelli, M.; Karthaus, W. R.; Hess, J.; Sigouros, M.; Donoghue, A.; Kossai, M.; Gao, D.; Cyrta, J.; Sailer, V.; Vosoughi, A.; Pauli, C.; Churakova, Y.; Cheung, C.; Deonarine, L. D.; McNary, T. J.; Rosati, R.; Tagawa, S. T.; Nanus, D. M.; Mosquera, J. M.; Sawyers, C. L.; Chen, Y.; Inghirami, G.; Rao, R. A.; Grandori, C.; Elemento, O.; Sboner, A.; Demichelis, F.; Rubin, M. A.; Beltran, H., Patient derived organoids to model rare prostate cancer phenotypes. *Nat Commun* **2018**, *9*, (1), 2404.
  32. Beshiri, M. L.; Tice, C. M.; Tran, C.; Nguyen, H. M.; Sowalsky, A. G.; Agarwal, S.; Jansson, K. H.; Yang, Q.; McGowen, K. M.; Yin, J.; Alilin, A. N.; Karzai, F. H.; Dahut, W. L.; Corey, E.; Kelly, K., A PDX/Organoid Biobank of Advanced Prostate Cancers Captures Genomic and Phenotypic Heterogeneity for Disease Modeling and Therapeutic Screening. *Clin Cancer Res* **2018**, *24*, (17), 4332-4345.
  33. Neeb, A.; Herranz, N.; Arce-Gallego, S.; Miranda, S.; Buroni, L.; Yuan, W.; Athie, A.; Casals, T.; Carmichael, J.; Rodrigues, D. N.; Gurel, B.; Rescigno, P.; Rekowski, J.; Welti, J.; Riisnaes, R.; Gil, V.; Ning, J.; Wagner, V.; Casanova-Salas, I.; Cordoba, S.; Castro, N.; Fenor de la Maza, M. D.; Seed, G.; Chandran, K.; Ferreira, A.; Figueiredo, I.; Bertan, C.; Bianchini, D.; Aversa, C.; Paschalidis, A.; Gonzalez, M.; Morales-Barrera, R.; Suarez, C.; Carles, J.; Swain, A.; Sharp, A.; Gil, J.; Serra, V.; Lord, C.; Carreira, S.; Mateo, J.; de Bono, J. S., Advanced Prostate Cancer with ATM Loss: PARP and ATR Inhibitors. *Eur Urol* **2021**, *79*, (2), 200-211.
  34. Moutal, A.; Martin, L. F.; Boinon, L.; Gomez, K.; Ran, D.; Zhou, Y.; Stratton, H. J.; Cai, S.; Luo, S.; Gonzalez, K. B.; Perez-Miller, S.; Patwardhan, A.; Ibrahim, M. M.; Khanna, R., SARS-CoV-2 Spike protein co-opts VEGF-A/Neuropilin-1 receptor signaling to induce analgesia. *Pain* **2020**.
  35. Ha, S.; Iqbal, N. J.; Mita, P.; Ruoff, R.; Gerald, W. L.; Lepor, H.; Taneja, S. S.; Lee, P.; Melamed, J.; Garabedian, M. J.; Logan, S. K., Phosphorylation of the androgen receptor by PIM1 in hormone refractory prostate cancer. *Oncogene* **2013**, *32*, (34), 3992-4000.
  36. Linn, D. E.; Yang, X.; Xie, Y.; Alfano, A.; Deshmukh, D.; Wang, X.; Shimelis, H.; Chen, H.; Li, W.; Xu, K.; Chen, M.; Qiu, Y., Differential regulation of androgen receptor by PIM-1 kinases via phosphorylation-dependent recruitment of distinct ubiquitin E3 ligases. *J Biol Chem* **2012**, *287*, (27), 22959-68.
  37. Markou, A.; Tzanikou, E.; Strati, A.; Zavridou, M.; Mastoraki, S.; Bournakis, E.; Lianidou, E., Is Overexpressed at a High Frequency in Circulating Tumor Cells from Metastatic Castration-Resistant Prostate Cancer Patients. *Cancers (Basel)* **2020**, *12*, (5).
  38. Tomura, M.; Sakaue-Sawano, A.; Mori, Y.; Takase-Utsugi, M.; Hata, A.; Ohtawa, K.; Kanagawa, O.; Miyawaki, A., Contrasting quiescent G0 phase with mitotic cell cycling in the mouse immune system. *PLoS One* **2013**, *8*, (9), e73801.
  39. Debnath, J.; Brugge, J. S., Modelling glandular epithelial cancers in three-dimensional cultures. *Nat Rev Cancer* **2005**, *5*, (9), 675-88.
  40. Lee, S.; Burner, D. N.; Mendoza, T. R.; Muldong, M. T.; Arreola, C.; Wu, C. N.; Cacalano, N. A.; Kulidjian, A. A.; Kane, C. J.; Jamieson, C. A. M., Establishment and Analysis of Three-Dimensional (3D) Organoids Derived from Patient Prostate Cancer Bone Metastasis Specimens and their Xenografts. *J Vis Exp* **2020**, (156).
  41. Pappas, K. J.; Choi, D.; Sawyers, C. L.; Karthaus, W. R., Prostate Organoid Cultures as Tools to Translate Genotypes and Mutational Profiles to Pharmacological Responses. *J Vis Exp* **2019**, (152).
  42. Crowell, P. D.; Giafaglione, J. M.; Hashimoto, T.; Diaz, J. A.; Goldstein, A. S., Evaluating the Differentiation Capacity of Mouse Prostate Epithelial Cells Using Organoid Culture. *J Vis Exp* **2019**, (153).
  43. Hu, W. Y.; Hu, D. P.; Xie, L.; Birch, L. A.; Prins, G. S., Isolation of Stem-like Cells from 3-Dimensional Spheroid Cultures. *J Vis Exp* **2019**, (154).
  44. Fatehullah, A.; Tan, S. H.; Barker, N., Organoids as an in vitro model of human development and disease. *Nat Cell Biol* **2016**, *18*, (3), 246-54.
  45. van Leenders, G. J.; Gage, W. R.; Hicks, J. L.; van Balken, B.; Aalders, T. W.; Schalken, J. A.; De Marzo, A. M., Intermediate cells in human prostate epithelium are enriched in proliferative inflammatory atrophy. *Am J Pathol* **2003**, *162*, (5), 1529-37.
  46. Linxweiler, J.; Körbel, C.; Müller, A.; Hammer, M.; Veith, C.; Bohle, R. M.; Stöckle, M.; Junker, K.; Menger, M. D.; Saar, M., A novel mouse model of human prostate cancer to study intraprostatic tumor growth and the development of lymph node metastases. *Prostate* **2018**, *78*, (9), 664-675.
  47. Liu, X.; Grogan, T. R.; Hieronymus, H.; Hashimoto, T.; Mottahedeh, J.; Cheng, D.; Zhang, L.; Huang, K.; Stoyanova, T.; Park, J. W.; Shkhyan, R. O.; Nowroozizadeh, B.; Rettig, M. B.; Sawyers, C. L.; Elashoff, D.; Horvath, S.; Huang, J.; Witte, O. N.; Goldstein, A. S., Low CD38 Identifies Progenitor-like Inflammation-Associated Luminal Cells that Can Initiate Human Prostate Cancer and Predict Poor Outcome. *Cell Rep* **2016**, *17*, (10), 2596-2606.

48. Kröger, C.; Afeyan, A.; Mraz, J.; Eaton, E. N.; Reinhardt, F.; Khodor, Y. L.; Thiru, P.; Bierie, B.; Ye, X.; Burge, C. B.; Weinberg, R. A., Acquisition of a hybrid E/M state is essential for tumorigenicity of basal breast cancer cells. *Proc Natl Acad Sci U S A* **2019**, 116, (15), 7353-7362.
49. Karthaus, W. R.; Hofree, M.; Choi, D.; Linton, E. L.; Turkekul, M.; Bejnood, A.; Carver, B.; Gopalan, A.; Abida, W.; Laudone, V.; Biton, M.; Chaudhary, O.; Xu, T.; Masilionis, I.; Manova, K.; Mazutis, L.; Pe'er, D.; Regev, A.; Sawyers, C. L., Regenerative potential of prostate luminal cells revealed by single-cell analysis. *Science* **2020**, 368, (6490), 497-505.
50. Lowrance, W. T.; Breau, R. H.; Chou, R.; Chapin, B. F.; Crispino, T.; Dreicer, R.; Jarrard, D. F.; Kibel, A. S.; Morgan, T. M.; Morgans, A. K.; Oh, W. K.; Resnick, M. J.; Zietman, A. L.; Cookson, M. S., Advanced Prostate Cancer: AUA/ASTRO/SUO Guideline PART I. *J Urol* **2021**, 205, (1), 14-21.
51. Goff, D. J.; Court Recart, A.; Sadarangani, A.; Chun, H. J.; Barrett, C. L.; Krajewska, M.; Leu, H.; Low-Marchelli, J.; Ma, W.; Shih, A. Y.; Wei, J.; Zhai, D.; Geron, I.; Pu, M.; Bao, L.; Chuang, R.; Balaian, L.; Gotlib, J.; Minden, M.; Martinelli, G.; Rusert, J.; Dao, K. H.; Shazand, K.; Wentworth, P.; Smith, K. M.; Jamieson, C. A.; Morris, S. R.; Messer, K.; Goldstein, L. S.; Hudson, T. J.; Marra, M.; Frazer, K. A.; Pellecchia, M.; Reed, J. C.; Jamieson, C. H., A Pan-BCL2 inhibitor renders bone-marrow-resident human leukemia stem cells sensitive to tyrosine kinase inhibition. *Cell Stem Cell* **2013**, 12, (3), 316-28.
52. Morrissey, C.; Vessella, R. L.; Lange, P. H.; Lam, H. M., The biology and clinical implications of prostate cancer dormancy and metastasis. *J Mol Med (Berl)* **2016**, 94, (3), 259-65.
53. Wu, Y.; Schoenborn, J. R.; Morrissey, C.; Xia, J.; Larson, S.; Brown, L. G.; Qu, X.; Lange, P. H.; Nelson, P. S.; Vessella, R. L.; Fang, M., High-Resolution Genomic Profiling of Disseminated Tumor Cells in Prostate Cancer. *J Mol Diagn* **2016**, 18, (1), 131-43.
54. Chéry, L.; Lam, H. M.; Coleman, I.; Lakely, B.; Coleman, R.; Larson, S.; Aguirre-Ghiso, J. A.; Xia, J.; Gulati, R.; Nelson, P. S.; Montgomery, B.; Lange, P.; Snyder, L. A.; Vessella, R. L.; Morrissey, C., Characterization of single disseminated prostate cancer cells reveals tumor cell heterogeneity and identifies dormancy associated pathways. *Oncotarget* **2014**, 5, (20), 9939-51.
55. Dhimolea, E.; de Matos Simoes, R.; Kansara, D.; Al'Khafaji, A.; Bouyssou, J.; Weng, X.; Sharma, S.; Raja, J.; Awate, P.; Shirasaki, R.; Tang, H.; Glassner, B. J.; Liu, Z.; Gao, D.; Bryan, J.; Bender, S.; Roth, J.; Scheffer, M.; Jeselsohn, R.; Gray, N. S.; Georgakoudi, I.; Vazquez, F.; Tsherniak, A.; Chen, Y.; Welm, A.; Duy, C.; Melnick, A.; Bartholdy, B.; Brown, M.; Culhane, A. C.; Mitsiades, C. S., An Embryonic Diapause-like Adaptation with Suppressed Myc Activity Enables Tumor Treatment Persistence. *Cancer Cell* **2021**, 39, (2), 240-256.e11.
56. Pineda, G.; Lennon, K. M.; Delos Santos, N. P.; Lambert-Fliszar, F.; Riso, G. L.; Lazzari, E.; Marra, M. A.; Morris, S.; Sakaue-Sawano, A.; Miyawaki, A.; Jamieson, C. H., Tracking of Normal and Malignant Progenitor Cell Cycle Transit in a Defined Niche. *Sci Rep* **2016**, 6, 23885.
57. Vummidi Giridhar, P.; Williams, K.; VonHandorf, A. P.; Deford, P. L.; Kasper, S., Constant Degradation of the Androgen Receptor by MDM2 Conserves Prostate Cancer Stem Cell Integrity. *Cancer Res* **2019**, 79, (6), 1124-1137.
58. Hoffmann, M.; Kleine-Weber, H.; Schroeder, S.; Krüger, N.; Herrler, T.; Erichsen, S.; Schiergens, T. S.; Herrler, G.; Wu, N. H.; Nitsche, A.; Müller, M. A.; Drosten, C.; Pöhlmann, S., SARS-CoV-2 Cell Entry Depends on ACE2 and TMPRSS2 and Is Blocked by a Clinically Proven Protease Inhibitor. *Cell* **2020**, 181, (2), 271-280.e8.
59. Qiao, Y.; Wang, X. M.; Mannan, R.; Pitchiaya, S.; Zhang, Y.; Wotring, J. W.; Xiao, L.; Robinson, D. R.; Wu, Y. M.; Tien, J. C.; Cao, X.; Simko, S. A.; Apel, I. J.; Bawa, P.; Kregel, S.; Narayanan, S. P.; Raskind, G.; Ellison, S. J.; Parolia, A.; Zelenka-Wang, S.; McMurry, L.; Su, F.; Wang, R.; Cheng, Y.; Delekta, A. D.; Mei, Z.; Pretto, C. D.; Wang, S.; Mehra, R.; Sexton, J. Z.; Chinnaiyan, A. M., Targeting transcriptional regulation of SARS-CoV-2 entry factors. *Proc Natl Acad Sci U S A* **2020**.
60. Moradi, F.; Enjezab, B.; Ghadiri-Anari, A., The role of androgens in COVID-19. *Diabetes Metab Syndr* **2020**, 14, (6), 2003-2006.
61. Baratchian, M.; McManus, J. M.; Berk, M.; Nakamura, F.; Mukhopadhyay, S.; Xu, W.; Erzurum, S.; Drazba, J.; Peterson, J.; Klein, E. A.; Gaston, B.; Sharifi, N., Sex, androgens and regulation of pulmonary AR, TMPRSS2 and ACE2. *bioRxiv* **2020**.
62. Avanzato, V. A.; Matson, M. J.; Seifert, S. N.; Pryce, R.; Williamson, B. N.; Anzick, S. L.; Barbian, K.; Judson, S. D.; Fischer, E. R.; Martens, C.; Bowden, T. A.; de Wit, E.; Riedo, F. X.; Munster, V. J., Case Study: Prolonged Infectious SARS-CoV-2 Shedding from an Asymptomatic Immunocompromised Individual with Cancer. *Cell* **2020**, 183, (7), 1901-1912.e9.
63. Montopoli, M.; Zumerle, S.; Vettor, R.; Rugge, M.; Zorzi, M.; Catapano, C. V.; Carbone, G. M.; Cavalli, A.; Pagano, F.; Ragazzi, E.; Prayer-Galetti, T.; Alimonti, A., Androgen-deprivation therapies for prostate cancer and risk of infection by SARS-CoV-2: a population-based study (N = 4532). *Ann Oncol* **2020**, 31, (8), 1040-1045.
64. Bhowmick, N. A.; Oft, J.; Dorff, T.; Pal, S.; Agarwal, N.; Figlin, R. A.; Posadas, E. M.; Freedland, S. J.; Gong, J., COVID-19 and androgen-targeted therapy for prostate cancer patients. *Endocr Relat Cancer* **2020**, 27, (9), R281-R292.
65. Ghazizadeh, Z.; Majd, H.; Richter, M.; Samuel, R.; Zekavat, S. M.; Asgharian, H.; Farahvashi, S.; Kalantari, A.; Ramirez, J.; Zhao, H.; Natarajan, P.; Goodarzi, H.; Fattah, F., Androgen Regulates SARS-CoV-2 Receptor Levels and Is Associated with Severe COVID-19 Symptoms in Men. *bioRxiv* **2020**.
66. Han, Y.; Duan, X.; Yang, L.; Nilsson-Payant, B. E.; Wang, P.; Duan, F.; Tang, X.; Yaron, T. M.; Zhang, T.; Uhl, S.; Bram, Y.; Richardson, C.; Zhu, J.; Zhao, Z.; Redmond, D.; Houghton, S.; Nguyen, D. T.; Xu, D.; Wang, X.; Jessurun, J.; Borczuk, A.; Huang, Y.; Johnson, J. L.; Liu, Y.; Xiang, J.; Wang, H.; Cantley, L. C.; tenOever, B. R.; Ho, D. D.; Pan, F. C.; Evans, T.; Chen, H. J.; Schwartz, R. E.; Chen, S., Identification of SARS-CoV-2 inhibitors using lung and colonic organoids. *Nature* **2021**, 589, (7841), 270-275.
67. Salahudeen, A. A.; Choi, S. S.; Rustagi, A.; Zhu, J.; van Unen, V.; de la O, S. M.; Flynn, R. A.; Margalef-Català, M.; Santos, A. J. M.; Ju, J.; Batish, A.; Usui, T.; Zheng, G. X. Y.; Edwards, C. E.; Wagar, L. E.; Luca, V.; Anchang, B.; Nagendran, M.; Nguyen, K.; Hart, D. J.; Terry, J. M.; Belgrader, P.; Ziraldo, S. B.; Mikkelsen, T. S.; Harbury, P. B.; Glenn, J. S.; Garcia, K. C.; Davis, M. M.; Baric, R. S.; Sabatti, C.; Amieva, M. R.; Blish, C. A.; Desai, T. J.; Kuo, C. J., Progenitor identification and SARS-CoV-2 infection in human distal lung organoids. *Nature* **2020**, 588, (7839), 670-675.

68. Hirata, T.; Park, S. C.; Muldong, M. T.; Wu, C. N.; Yamaguchi, T.; Strasner, A.; Raheem, O.; Kumon, H.; Sah, R. L.; Cacalano, N. A.; Jamieson, C. H. M.; Kane, C. J.; Masuda, K.; Kulidjian, A. A.; Jamieson, C. A. M., Specific bone region localization of osteolytic versus osteoblastic lesions in a patient-derived xenograft model of bone metastatic prostate cancer. *Asian J Urol* **2016**, *3*, (4), 229-239.
69. Langmead, B.; Salzberg, S. L., Fast gapped-read alignment with Bowtie 2. *Nat Methods* **2012**, *9*, (4), 357-9.
70. Trapnell, C.; Roberts, A.; Goff, L.; Pertea, G.; Kim, D.; Kelley, D. R.; Pimentel, H.; Salzberg, S. L.; Rinn, J. L.; Pachter, L., Differential gene and transcript expression analysis of RNA-seq experiments with TopHat and Cufflinks. *Nat Protoc* **2012**, *7*, (3), 562-78.
71. Li, H.; Handsaker, B.; Wysoker, A.; Fennell, T.; Ruan, J.; Homer, N.; Marth, G.; Abecasis, G.; Durbin, R.; Subgroup, G. P. D. P., The Sequence Alignment/Map format and SAMtools. *Bioinformatics* **2009**, *25*, (16), 2078-9.
72. Subramanian, A.; Tamayo, P.; Mootha, V. K.; Mukherjee, S.; Ebert, B. L.; Gillette, M. A.; Paulovich, A.; Pomeroy, S. L.; Golub, T. R.; Lander, E. S.; Mesirov, J. P., Gene set enrichment analysis: a knowledge-based approach for interpreting genome-wide expression profiles. *Proc Natl Acad Sci U S A* **2005**, *102*, (43), 15545-50.
73. Hu, W. Y.; Hu, D. P.; Xie, L.; Li, Y.; Majumdar, S.; Nonn, L.; Hu, H.; Shioda, T.; Prins, G. S., Isolation and functional interrogation of adult human prostate epithelial stem cells at single cell resolution. *Stem Cell Res* **2017**, *23*, 1-12.
74. Moad, M.; Hannezo, E.; Buczacki, S. J.; Wilson, L.; El-Sherif, A.; Sims, D.; Pickard, R.; Wright, N. A.; Williamson, S. C.; Turnbull, D. M.; Taylor, R. W.; Greaves, L.; Robson, C. N.; Simons, B. D.; Heer, R., Multipotent Basal Stem Cells, Maintained in Localized Proximal Niches, Support Directed Long-Ranging Epithelial Flows in Human Prostates. *Cell Rep* **2017**, *20*, (7), 1609-1622.
75. Warrier, N. M.; Agarwal, P.; Kumar, P., Emerging Importance of Survivin in Stem Cells and Cancer: the Development of New Cancer Therapeutics. *Stem Cell Rev Rep* **2020**, *16*, (5), 828-852.
76. Adisetiyo, H.; Liang, M.; Liao, C. P.; Aycock-Williams, A.; Cohen, M. B.; Xu, S.; Neamati, N.; Conway, E. M.; Cheng, C. Y.; Nikitin, A. Y.; Roy-Burman, P., Loss of survivin in the prostate epithelium impedes carcinogenesis in a mouse model of prostate adenocarcinoma. *PLoS One* **2013**, *8*, (7), e69484.
77. Schroeder, A.; Herrmann, A.; Cherryholmes, G.; Kowollik, C.; Buettner, R.; Pal, S.; Yu, H.; Müller-Newen, G.; Jove, R., Loss of androgen receptor expression promotes a stem-like cell phenotype in prostate cancer through STAT3 signaling. *Cancer Res* **2014**, *74*, (4), 1227-37.
78. Sui, X.; Cai, J.; Li, H.; He, C.; Zhou, C.; Dong, Y.; Chen, L.; Zhang, B.; Wang, Y.; Zhang, Y.; Qiu, Y.; Zhao, Y.; Huang, Y.; Shen, Y.; Wu, H.; Xiao, J.; Mason, C.; Zhu, Q.; Han, S., p53-dependent CD51 expression contributes to characteristics of cancer stem cells in prostate cancer. *Cell Death Dis* **2018**, *9*, (5), 523.
79. Wang, L.; Li, Y.; Yang, X.; Yuan, H.; Li, X.; Qi, M.; Chang, Y. W.; Wang, C.; Fu, W.; Yang, M.; Zhang, J.; Han, B., ERG-SOX4 interaction promotes epithelial-mesenchymal transition in prostate cancer cells. *Prostate* **2014**, *74*, (6), 647-58.
80. Miao, L.; Yang, L.; Li, R.; Rodrigues, D. N.; Crespo, M.; Hsieh, J. T.; Tilley, W. D.; de Bono, J.; Selth, L. A.; Raj, G. V., Disrupting Androgen Receptor Signaling Induces Snail-Mediated Epithelial-Mesenchymal Plasticity in Prostate Cancer. *Cancer Res* **2017**, *77*, (11), 3101-3112.
81. Carafa, V.; Altucci, L.; Nebbioso, A., Dual Tumor Suppressor and Tumor Promoter Action of Sirtuins in Determining Malignant Phenotype. *Front Pharmacol* **2019**, *10*, 38.
82. Linn, D. E.; Yang, X.; Sun, F.; Xie, Y.; Chen, H.; Jiang, R.; Chumsri, S.; Burger, A. M.; Qiu, Y., A Role for OCT4 in Tumor Initiation of Drug-Resistant Prostate Cancer Cells. *Genes Cancer* **2010**, *1*, (9), 908-16.
83. Jeter, C. R.; Liu, B.; Liu, X.; Chen, X.; Liu, C.; Calhoun-Davis, T.; Repass, J.; Zaehres, H.; Shen, J. J.; Tang, D. G., NANOG promotes cancer stem cell characteristics and prostate cancer resistance to androgen deprivation. *Oncogene* **2011**, *30*, (36), 3833-45.
84. Koh, C. M.; Bieberich, C. J.; Dang, C. V.; Nelson, W. G.; Yegnasubramanian, S.; De Marzo, A. M., MYC and Prostate Cancer. *Genes Cancer* **2010**, *1*, (6), 617-28.
85. Bae, K. M.; Parker, N. N.; Dai, Y.; Vieweg, J.; Siemann, D. W., E-cadherin plasticity in prostate cancer stem cell invasion. *Am J Cancer Res* **2011**, *1*, (1), 71-84.
86. Putzke, A. P.; Ventura, A. P.; Bailey, A. M.; Akture, C.; Opoku-Ansah, J.; Celiktaş, M.; Hwang, M. S.; Darling, D. S.; Coleman, I. M.; Nelson, P. S.; Nguyen, H. M.; Corey, E.; Tewari, M.; Morrissey, C.; Vessella, R. L.; Knudsen, B. S., Metastatic progression of prostate cancer and e-cadherin regulation by zeb1 and SRC family kinases. *Am J Pathol* **2011**, *179*, (1), 400-10.
87. Lukacs, R. U.; Memarzadeh, S.; Wu, H.; Witte, O. N., Bmi-1 is a crucial regulator of prostate stem cell self-renewal and malignant transformation. *Cell Stem Cell* **2010**, *7*, (6), 682-93.
88. Schneider, J. A.; Logan, S. K., Revisiting the role of Wnt/β-catenin signaling in prostate cancer. *Mol Cell Endocrinol* **2018**, *462*, (Pt A), 3-8.
89. Lee, E.; Madar, A.; David, G.; Garabedian, M. J.; Dasgupta, R.; Logan, S. K., Inhibition of androgen receptor and β-catenin activity in prostate cancer. *Proc Natl Acad Sci U S A* **2013**, *110*, (39), 15710-5.
90. Li, P.; Yang, R.; Gao, W. Q., Contributions of epithelial-mesenchymal transition and cancer stem cells to the development of castration resistance of prostate cancer. *Mol Cancer* **2014**, *13*, 55.